Theory of Precipitation of Protein Mixtures by Nonionic Polymer

Hari Mahadevan and Carol K. Hall
Dept. of Chemical Engineering, North Carolina State University, Raleigh, NC 27695

A theory is developed to predict the solubility of protein mixtures in solutions containing nonionic polymer. Effective protein-protein interactions due to polymer are taken to be volume-exclusion potentials derived using statistical mechanics. Statistical-mechanical perturbation theory is used to calculate chemical potentials. The effects of protein size, mole fraction and polymer concentration on solubility are explored. The theory is extended to include electrostatic interactions. The excess chemical potential of the proteins due to the charges on all species is calculated using the mean spherical approximation for a mixture of charged hard spheres. The theory predicts: the larger protein is preferentially precipitated over the smaller one; the more concentrated protein is more likely to precipitate; and increasing the charge of a particular protein reduces its ability to precipitate.

Introduction

Protein precipitation is the oldest practical way to separate different proteins from a solution mixture (Bjurstrom, 1985). In spite of the age of the technique, precipitation procedures remain a popular route to separate proteins, particularly for the coarse separations involved in the first step of a purification train (Scopes, 1982). A variety of precipitating agents have been used to elicit proteins out of solution. These include inorganic salts, organic solvents, nonionic polymer, and polyelectrolytes. In this article we discuss a fundamental approach to modeling the precipitation of mixtures of proteins by the addition of nonionic polymer.

The addition of nonionic polymers to precipitate proteins is a well-established technique with high-molecular-weight polymers of polyethylene glycol (PEG) being used both in the laboratory and in pilot plant scale (Bjurstrom, 1985) to accomplish the precipitation. A major advantage of this technique is that it can be done at ambient temperatures, because the polymer does not significantly interact with the protein. Also, relatively low concentrations of polymer, on the order of 5–15 wt. %, are required to precipitate most proteins. There is, however, a tendency for the polymer to contaminate the precipitate, although it has been found that using PEG of a higher average molecular weight significantly reduces this contamination (Knoll and Hermans, 1983).

A variety of researchers have studied the solubility of single proteins in solutions containing polymer. Kula et al. (1976), Middaugh et al. (1979), Ingham et al. (1977, 1978), Atha and Ingham (1981), and Haire and coworkers (1984) have measured apparent solubilities and thermodynamic properties of various proteins in the presence of nonionic polymers using a variety of experimental techniques. Most studies have generated precipitation curves that relate protein solubility to polymer concentration. The most significant result of these studies is the consensus that specific chemical interactions between protein and polymer are *absent*. This has led to the conclusion that the primary mechanism for phase separation in these systems is steric hindrance (also called volume exclusion). Polson et al. (1964) have examined the precipitation of protein mixtures by PEG and found ranges of polymer concentrations where proteins of different sizes precipitated, the general rule being that the larger polymers precipitated at lower PEG concentrations.

Most of the theories described in the literature of polymer-induced protein precipitation are based on the thermodynamic theories of Ogston and Phelps (1961), Ogston (1962) and Edmond and Ogston (1968). Central to these approaches is the idea that steric hindrance is the primary mechanism by which a nonionic polymer induces phase separation in a protein so-

Correspondence concerning this article should be addressed to C. K. Hall.
H. Mahadevan is currently at Merck Sharp and Dohme Research Laboratories, P. O. Box 2000, Rahway, NJ 07065.

lution. In other words, although the intrinsic solubility of a protein in solution depends on pH, ionic strength and other protein-specific parameters, the addition of nonionic polymer to a protein solution decreases protein solubility by sterically excluding protein from regions of the solvent it normally occupies, thereby concentrating the protein until its solubility is exceeded and precipitation occurs (Polson et al., 1964; Knoll and Hermans, 1983). Most theories developed by applying these arguments can predict only a few of the experimentally observed trends.

In an earlier article (Mahadevan and Hall, 1990), we proposed a fundamental theory based on the work of Gast et al. (1983) to explain the precipitation of *pure* proteins (single-protein systems) by nonionic polymer. We were able to correctly predict the trends observed in the solubility resulting from changes in all the process variables: the pH, ionic strength and protein and polymer molecular weights. We presented the results for precipitation in the form of solubility curves, relating the log of the solubility to the polymer concentration for varying protein-polymer diameter ratios and for different pHs and ionic strengths.

In this article, we extend the theory to solutions containing mixtures of proteins and examine the effect of excluded volume on protein solubility in the presence of polymer, including charge-related effects. A fundamental approach is used to predict the solubility of proteins in binary mixtures of different mole fractions. An important focus is to predict which protein (large or small) will precipitate in solutions containing nonionic polymer. We calculate the solubilities for varying diameter ratios of protein 1: protein 2: polymer and for various polymer concentrations. In studying the size-related effects, the theory predicts that the larger protein is preferentially precipitated over the smaller one. The theory provides an insight into the competition between the "concentration effect" that favors the precipitation of the more concentrated protein and the "size effect" that favors the precipitation of the larger protein. The theory also predicts that the precipitation of the larger protein is increasingly favored with an increase both in the concentration of the polymer and in the diameter ratio between proteins.

Finally, we find that for a fixed diameter ratio between proteins the solubility decreases with increasing concentration of polymer. In our exploration of electrostatic effects, we find that increasing the charge on a protein reduces its ability to precipitate. We maintain the size ratio fixed at 6:5:1. Keeping the two proteins at fairly equal sizes minimizes the contribution of the size effect (which is the primary driving force in the precipitation of proteins by polymer) and allows us to make comparison with the results obtained for this particular size ratio. We find that for the size ratio studied, size and charge are equally important criteria in determining the phase transition behavior of these systems and that protein charge also plays an important role in determining whether a particular protein can be elicited out of solution. Increasing the size and relative concentration (mole fraction) of a particular protein increases its tendency to precipitate, while increasing the charge reduces its tendency to precipitate. We present examples in support of these conclusions.

First, we develop the model for the polymer-induced precipitation of protein mixtures which interact via excluded-volume interactions only. The theory's predictions are then described, followed by a discussion of the results and an evaluation of the assumptions made. Expressions for the excluded volume intermolecular potential used are derived in the Appendix. Subsequently, we incorporate electrostatic effects into the model. We also describe how the mean spherical approximation (MSA) may be used to calculate the electrostatic contribution to the chemical potential of various species. The model is used to predict protein solubility of charged-protein systems in the presence of nonionic polymer. The results of this model are described as well as the relative importance of size and charge in these systems.

Development of Theory: Size-Related Effects

In this section we extend the theory of polymer-induced precipitation of single proteins by Mahadevan and Hall (1990) to binary mixtures of proteins.

Molecular model

Our treatment of the polymer-induced precipitation of protein mixtures begins with a model for the interaction potential. In parallel with our previous work, we will treat the protein 1-protein 2-polymer-water system as a pseudo two-component system. The justification for this reduction is due to McMillan and Mayer (1945), who developed a solution theory showing that the expansion methods of imperfect gas theory could be applied to liquid solutions, with solute-solute potentials of mean force determined by averaging over the positions and coordinates of the solvent molecules, provided that the solution was under an additional pressure, Π (the osmotic pressure). Essentially, this implies that the potential of mean force between solute molecules can be interpreted independent of solvent composition, provided that the constraint of the additional pressure is imposed on the system. The solvent (single or multicomponent), therefore, does not play an explicit role in the determination of the partition function (or thermodynamic properties). In particular, for our system, the roles of the polymer and water are averaged out and we treat the system as a pseudo two-component system, the two components being the two protein species. We derive below an expression for the effective interaction or, more precisely, the potential of mean force between protein molecules in the presence of a solvent, polymer, plus water.

To calculate the potential of mean force, we model the protein molecules as hard spheres of diameter d_1 and d_2, and the polymer molecules as spheres of diameter d_3 that can penetrate each other but not the protein molecules. The aqueous medium is modeled as a continuum. We employ the convention that protein 1 is the larger protein. The effect of added polymer is included via an excluded-volume attraction between proteins in polymer solution that arises in the following way. Around each protein molecule is a shell of thickness $d_3/2$ which excludes all polymer molecules. When polymer is absent or when protein molecules are apart far enough, the protein molecules do not feel the presence of one another. However, when they are close enough together such that polymer cannot enter the space between the protein molecules, an unbalanced osmotic force due to the surrounding polymer molecules is created, tending to push the protein molecules together. The induced attraction between proteins due to this phenomenon is called the volume-

exclusion attraction. This attraction is the potential of mean force between the protein molecules in the presence of polymer.

Expressions for the volume-exclusion attraction have been derived based on geometrical considerations by Asakura and Oosawa (1958) and later rederived by de Hek and Vrij (1981). This potential, however, was for a single-component fluid, valid in our context only for single-protein systems. For protein mixtures, however, in addition to the attraction felt between like proteins due to the polymer, there is an attraction between *unlike* proteins, which is not accounted for in the Asakura-Oosawa potential. In the Appendix, we derive a general volume-exclusion potential for binary systems using statistical-mechanical arguments as an effective interaction between particles in a background fluid (Dickman, 1990). For identical particles (molecules), this potential reduces to the Asakura-Oosawa potential.

The forms for the intermolecular potentials (actually potentials of mean force) are as follows, for $i=1,2$:

$$u_{ii}^{\text{vex}}(r) = \begin{cases} \infty, & r < d_i \\ -\dfrac{4\pi n_3}{2} d_{i3}^3 \left[1 - \dfrac{3r}{4d_{i3}} + \dfrac{r^3}{16 d_{i3}^3} \right], & d_i \le r \le d_i + d_3 \\ 0, & d_i + d_3 < r \end{cases} \quad (1)$$

Also,

$$u_{ij}^{\text{vex}}(r) = \begin{cases} \infty, & r < \dfrac{d_1 + d_2}{2} \\ -\dfrac{2\pi n_3}{3} \{ d_{13}^3 + d_{23}^3 \} \left[1 - \dfrac{3}{4} \dfrac{\{ d_{13}^2 + d_{23}^2 \}}{\{ d_{13}^3 + d_{23}^3 \}} r + \dfrac{r^3}{8\{ d_{13}^2 - d_{23}^2 \}} - \dfrac{3}{8r} \dfrac{\{ d_{13}^3 - d_{23}^2 \}^2}{\{ d_{13}^3 + d_{23}^3 \}} \right], & \dfrac{d_1 + d_2}{2} < r < \dfrac{d_1 + d_2 + 2d_3}{2} \\ 0, & r > \dfrac{d_1 + d_2 + 2d_3}{2} \end{cases} \quad (2)$$

In Eqs. 1 and 2, d_i is the diameter of species i, d_{ij} is $(d_i + d_j)/2$, n_3 is the number density of polymer molecules in the polymer solution (that is, in the absence of protein), r is the distance of separation between centers, k is Boltzmann's constant, and T is the absolute temperature. The intermolecular potential can be rewritten as a sum of a reference and a perturbing potential, thus rendering it useful for a perturbation analysis as described in the next subsection.

Perturbation theory

Perturbation theory is a method, based in statistical mechanics (McQuarrie, 1976), for predicting the thermodynamic properties of a system. In this method, the pairwise interaction potential is decomposed into a reference potential and a perturbing potential. The reference potential is chosen to represent a system with well-known thermodynamic properties. It must be as close as possible to the (real) system of interest, yet be simple enough to permit accurate calculations of the requisite properties in a chosen phase. Usually, the hard-sphere potential is chosen as the reference and the attraction is added on as the perturbing potential. If the calculations are performed in the canonical ensemble (constant number of particles N, volume V, and temperature T), the Helmholtz free energy A of the system under consideration can be obtained directly from the perturbation expansion. We employ the Leonard et al. perturbation theory (Leonard et al., 1970), which gives the Helmholtz free energy of a binary mixture in terms of the properties of a hard-sphere reference system. Leonard et al. derived expressions using both a pure and a multicomponent hard-sphere reference system. In this work, we employ the multicomponent system as our reference.

Expanding the Helmholtz free energy $A(\rho,x,T)$ to the first order yields (Leonard et al., 1970):

$$\frac{A - A_0}{NkT} = -4\pi\rho x_1 x_2 d_{12}^2 g_0^{12}(d_{12})[d_{12} - \delta_{12}] + \frac{2\pi}{\rho} \beta \sum_{ij} \rho_i \rho_j \int_{\sigma_{ij}}^{\infty} u_{ij}^{\text{vex}}(r) g_0^{ij}(r) r^2 dr. \quad (3)$$

where ρ is the sum of the number densities of molecules of component 1 and 2, x_1 and x_2 are the mole fractions, and g_0^{ij} and A_0 are the radial distribution function and the Helmholtz free energy of a reference mixture of hard spheres at the same density and mole fraction as the system under consideration. We discuss the calculation of these quantities in the following section. The terms $g_0^{12}(d_{12})$ and δ_{12} are defined as:

$$g_0^{12}(d_{12}) = \frac{1}{1-\psi} + \frac{3(\pi/6)\rho[x_1 d_{11}^2 + x_2 d_{22}^2]}{(1-\psi)^2} \frac{d_{11} d_{22}}{d_{11} + d_{22}} \quad (4)$$

where

$$\psi = (\pi/6)\rho[x_1 d_{11}^3 + x_2 d_{22}^3]$$

and

$$\delta_{12} = \int_0^{\sigma_{12}} [1 - \exp\{ -\beta u_{12}^{\text{vex}}(z) \}] dz \quad (5)$$

To predict phase transitions for the system it is necessary to calculate the chemical potentials μ_i of each species and the pressure, p, of the system (Gast et al., 1983; Mahadevan and Hall, 1990). These quantities can be calculated from the Helmholtz free energy as follows:

$$\frac{\mu_i}{kT} = \frac{1}{V} \left[\frac{\partial (A/kT)}{\partial \rho_i} \right]_{V,T,\rho_j} = \rho \left[\frac{\partial (A/NkT)}{\partial \rho_i} \right]_{V,T,\rho_j} + \frac{A}{NkT} \quad (6)$$

$$\frac{p}{kT} = \frac{\rho}{V} \left[\frac{\partial A/kT}{\partial \rho} \right]_{T,N} = p_0 + \rho^2 \left[\frac{\partial (A_1/NkT)}{\partial \rho} \right]_{T,N} \quad (7)$$

where p_0 is the pressure of the reference state and A_1 is the first-order correction to the Helmholtz free energy of the reference state from Eq. 3. Once the intermolecular potentials are known and the properties of the reference state calculated, the chemical potentials of the species and the pressure can be obtained from the perturbation expansion.

To predict phase transitions it is necessary to perform the

calculations for both a fluid phase and a solid (precipitate) phase. We treat the fluid phase as a mixture of proteins. The solid phase, however, is assumed to be *pure*. In other words, each protein is assumed to precipitate into *its own solid phase*; we do not allow for a solid-phase mixture (what we shall call coprecipitation), thus permitting the calculation of the solid-phase free energies to be identical to that described by Mahadevan and Hall (1990). Thus, the free energies are calculated for one mixed fluid phase and *two* pure solid phases (protein 1 and protein 2), and a thermodynamic stability analysis is performed to decide which of the two species is actually at its solubility limit at the given conditions. The assumption of two pure solid phases is a key assumption, and the significance of the neglect of coprecipitation in this analysis is discussed later.

The calculation of the free energies in the various phases necessitates using different reference states for the perturbation expansion. For the fluid phase, we need to evaluate A_0, the free energy of a mixture of hard spheres, and $g_0^{ij}(r)$, the radial distribution function of the reference mixture. For the *two* precipitate phases we need to evaluate the free energy and the radial distribution of a hard-sphere solid.

Property evaluations in the reference state

Very good approximations are available for the pressure, the free energies, and the radial distribution function of the hard-sphere mixture fluid. Expressions are also available to calculate these quantities for a pure hard-sphere solid. The equations used to calculate these properties are described below. As mentioned in the preceding section, the reference state for the fluid phase is a mixture of hard spheres, and the reference state for the solid (precipitate) phase is a system of pure hard spheres.

Equations of State for the Hard-Sphere Mixture Reference System. Mansoori et al. (1971) have proposed an equation of state for the hard-sphere fluid mixture system. It is based on a straightforward extension to mixtures of the well-known Carnahan-Starling equation of state for hard spheres (1970). Mansoori et al. derive an expression for the excess Helmholtz free energy of the mixture as:

$$\frac{A-A^{id}}{NkT} = -\frac{3}{2}(1-y_1+y_2+y_3)+\frac{3y_2+2y_3}{1-\eta} + \frac{3}{2}\left[\frac{1-y_1-y_2-\frac{1}{3}y_3}{(1-\eta)^2}\right]+(y_3-1)\ln(1-\eta) \quad (8)$$

where the various parameters, y_1, y_2, and y_3, are defined as:

$$y_1 = \sum_{j>i=1}^{m} \Delta_{ij}\frac{(d_i+d_j)}{(d_id_j)^{0.5}}$$

$$y_2 = \sum_{j>i=1}^{m} \Delta_{ij}\sum_{k=1}^{m}\frac{\eta_k}{\eta}\frac{(d_id_j)^{0.5}}{d_k}$$

$$y_3 = \left[\sum_{i=1}^{m}\left(\frac{\eta_i}{\eta}\right)^{2/3} x_i^{1/3}\right]^3$$

with

$$\Delta_{ij} = \frac{(\eta_i\eta_j)^{0.5}}{\eta}\frac{(d_i-d_j)^2}{d_id_j}(x_ix_j)^{0.5}$$

Also, η (in Eq. 8) is defined as:

$$\eta = \sum_i \eta_i = \frac{\pi\rho}{6}\sum_i x_i d_i^3 \quad (9)$$

where ρ is the number density, and d_i and x_i are the hard-sphere diameter and the mole fraction, respectively, of component i. Note that the excess free energy in this case is defined as the excess over that of an ideal gas at the same *volume* and temperature. To obtain A_0, the ideal gas contribution is added to the excess energy obtained from Eq. 8.

The solid-phase free energies are calculated for two pure phases in a manner identical to that described in our earlier article; we do not present the details of the calculation here.

Radial Distribution Function for the Hard-Sphere Mixture Reference System. We obtain the radial distribution functions for the hard-sphere mixture using Perram's method (1975), wherein the Ornstein-Zernike equation is reformulated, enabling its conversion into a linear differential-difference form which can be solved numerically. Our code was verified by reproducing published correlation functions for test cases (Perram, 1975).

We use the analytical approximation derived by Weis and Kincaid (1977) for the solid-phase radial distribution function. These expressions for the equations of state and the distribution functions are then used in conjunction with Eq. 3 in the manner described below to generate phase diagrams for the system.

Calculation of solubility

Solubility calculations were performed for a binary protein system, which is completely defined when the diameter ratios of the two proteins to the polymer, d_1/d_3 and d_2/d_3, the mole fraction, x_1, of one of the proteins in the fluid phase and the volume fraction, $\phi_3=(\pi n_3 d_3^3)/6$, of the polymer *added* to the fluid are specified. For each set of these parameters, the fluid-phase Helmholtz free energy was calculated as a function of the total volume fraction of protein, $\phi=[(\pi\rho_1 d_1^3)/6] + [(\pi\rho_2 d_2^3)/6]$ using Eq. 3 where ρ_1 and ρ_2 are the number densities of components 1 and 2, respectively. The chemical potential of each species and the pressure were then determined numerically using Eqs. 6 and 7. As mentioned earlier, the solid-phase Helmholtz free energies were calculated for both solid phases in a manner identical to that described by Mahadevan and Hall (1990).

To determine which fluid-solid pair is at equilibrium, a phase equilibria and thermodynamic stability analysis were performed for each value of the polymer concentration, ϕ_3, and protein mole fraction, x_1, as outlined below. In the fluid phase, the chemical potentials of both species were calculated at discrete values of the total volume fraction of protein, ϕ. In the solid phase, the chemical potential of each protein was calculated for varying values of the individual volume fraction of each protein [$\phi_1=(\pi\rho_1 d_1^3)/6$ and $\phi_2=(\pi\rho_2 d_2^3)/6$]. Next, the chemical potentials of each species in the fluid and the two pure solid phases were plotted vs. the reduced pressure. This procedure leads to a series of plots similar to the four sets of μ_i/kT vs. p/kT curves shown in Figures 1a and 1b.

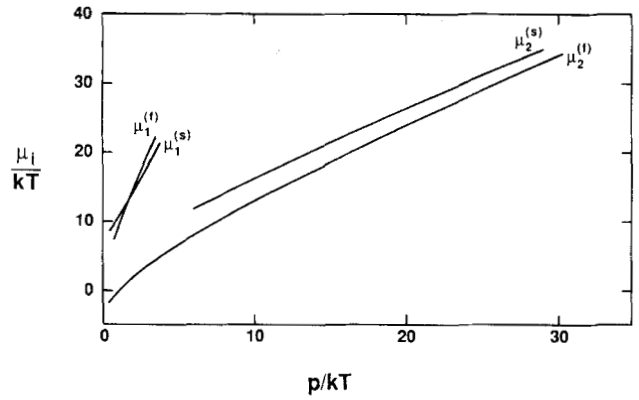

Figure 1a. Two sets of μ_i/kT vs. p/kT curves: single protein intersection.

The equilibrium between fluid and solid is determined by calculating the intersection of the fluid and solid μ_i/kT vs. p/kT curves for each species i. At the intersection point of these curves, the two phases are in equilibrium. If only one set of fluid-solid curves intersect, as in Figure 1a, then only the protein corresponding to that set precipitates. However, if both sets of curves intersect, as in Figure 1b, we can determine which protein precipitates by comparing the values of the pressure at the two intersection points (coexistence pressure), or by comparing the value of the total volume fraction at the two intersection points (since the pressure increases monotonically with the total protein volume fraction). The protein with the lower value of the coexistence pressure, or equivalently the lower value of the total protein volume fraction, precipitates. This volume fraction is called the coexistence volume fraction of total protein. Although the other protein does satisfy the phase equilibria criteria at a higher pressure according to the Gibbs phase rule, it does *not precipitate* at this pressure except at a unique point which can be called the "eutectic"—in analogy with freezing phase equilibria terminology (Sandler, 1988). This eutectic point corresponds to the case where the intersection of the two sets of curves (as in Figure 1b) occurs at the same pressure. As will be discussed in detail later, if at fixed values of ϕ_3 and T, one plots the phase diagram as pressure vs. mole fraction of protein 1, a typical freezing point

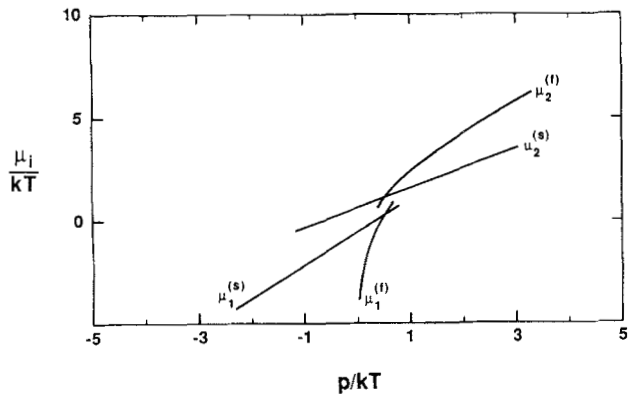

Figure 1b. Two sets of μ_i/kT vs. p/kT curves: both proteins intersect.

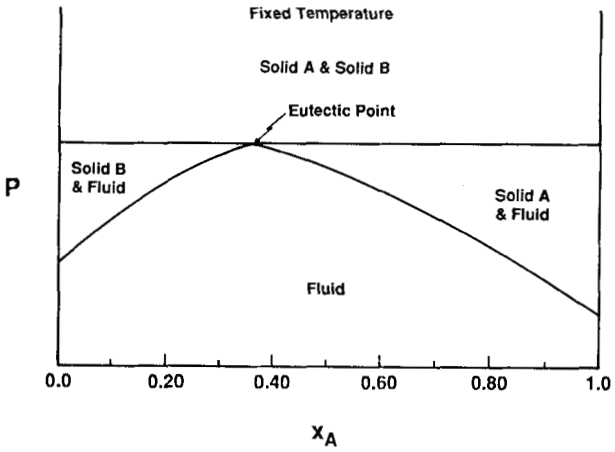

Figure 2. Phase diagram of fluid-solid equilibria when solids are pure components: formation of eutectic.

diagram as shown in Figure 2 is obtained; the eutectic is indicated on the diagram. Note that since we have interpreted the system containing the two proteins, polymer and water as a pseudo two-component system, the pressure, p, which appears in Eq. 7 is the osmotic pressure of a solution of two species in a two-component solvent, as per the McMillan-Mayer arguments described earlier. Also implicit in the pseudo two-component approach is the fact that the concentration of the polymer and water molecules around the protein molecules is equal in all phases.

Let us now examine in more detail the implications of the Gibbs phase rule for our pseudo two-component model (solvent averaged out, ϕ_3 fixed). When there are three phases in equilibrium (fluid, precipitate 1, and precipitate 2), we have 1 degree of freedom according to the Gibbs phase rule. Hence, at a fixed temperature, T, the values of the pressure, p, and the mole fraction, x_1, are fixed: the three phases will simultaneously exist only at a unique point, the eutectic. If we were to view the system as having three components (protein 1, protein 2, and polymer), then for three-phase equilibrium we would have 2 degrees of freedom. In this instance, fixing T and the chemical potential of the polymer would imply that the pressure and the mole fraction of the protein(s) were fixed, once again predicting the formation of a eutectic. We suspect that the eutectic-type behavior would also result, if we were to relax our assumption of pure solid phases and to allow coprecipitation (partially miscible solid phases). In this case, the phase diagram would resemble Figure 3. We are unable to model coprecipitation because of the lack of definitive information in the literature about a solid hard-sphere-mixture reference system.

The phase equilibria calculations proceed as follows. At fixed values of d_1/d_3, d_2/d_3, x_1, and ϕ_3, we calculate the free energies of the two proteins at incremental values of $\phi = \phi_1 + \phi_2$, starting at a low value (dilute protein solution). At each value of ϕ, a thermodynamic stability analysis is performed as described earlier to decide if either protein precipitates. If no precipitate is predicted, the total volume fraction is incremented until one of the two proteins precipitates. Repetition of these calculations for different polymer volume fractions, ϕ_3, and protein mole fractions, x_1, results in a phase diagram

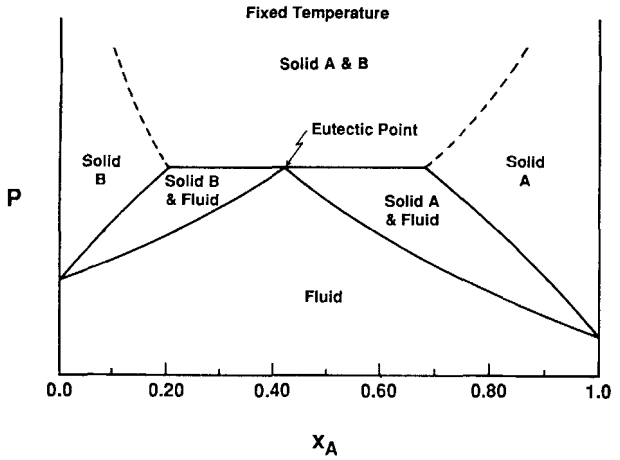

Figure 3. Phase diagram of fluid-solid equilibria with partial miscibility in solid state: formation of eutectic.

for one set of diameter ratios. Results have been obtained for four different diameter ratios of proteins to polymer.

To make a comparison with experimental data, which is typically plotted as log(Sol) (g/L) vs. % PEG (w/v), we need to convert the coexistence volume fractions of the individual proteins to solubilities. In our earlier article, we derived equations relating the fluid-phase coexistence volume fraction of a single protein to its solubility. This is readily extended to the solubility of a protein of species i in a mixture of proteins:

$$\log S_i(\text{g/L}) = \log\left[\frac{6{,}000\phi_i^{\text{coex}} M_i}{\pi d_i^3 N_{Av}}\right] \tag{10}$$

In our earlier article (1990), we also derived an expression for the polymer concentration in g/100 mL (or % polymer) in terms of the polymer number density, n_3, and the volume fractions of the precipitating proteins. For protein mixtures, this becomes:

$$\%\text{ polymer (g/100 mL)} = \frac{100 M_3 n_3 (1 - \Sigma_i \phi_i)}{N_{Av}} \tag{11}$$

where N_{Av} is Avogadro's number (used for conversion from molar to weight units). The solubility can also be rewritten in terms of $\overline{V}_i$, the partial specific volume of the protein, $\overline{V}_1$, the inverse specific density of water (solvent), and δ_1, which is defined to be the hydration (g H_2O/g protein).

$$\log S_i = \log\left[\frac{1{,}000\phi_i}{\overline{V}_i + \delta_1 \overline{V}_1}\right] \tag{12}$$

The advantage of using this formalism over that of directly incorporating the protein radii is that it is independent of the diameter-molecular weight correlation of a protein and that there are very specific ranges for the partial specific volumes and the hydration for globular proteins. Virtually all proteins have $\overline{V}_i$ values between 0.69 and 0.75 cm^3/g, so long as they do not have extensive material other than amino acids in their composition (Cantor and Schimmel, 1980). Also hydration values between 0.3 and 0.4 g H_2O/g protein are typical for globular proteins. In this article, we use Eq. 12 to calculate the solubilities with representative values of 0.72 for $\overline{V}_2$ and $\overline{V}_3$ and 0.35 for δ_1.

Solubility calculations were performed for 4 protein-polymer diameter ratios. For each diameter ratio, 9 different protein mole fraction mixtures were studied ($x_1 = 0.0$, 0.05, 0.10, 0.30, 0.50, 0.70, 0.90, 0.95, and 1.0). For the 6:5:1 case, additional mole fractions of 0.15 and 0.20 were studied. Protein 1 was always taken to be the larger protein. For each mole fraction mixture, the solubility analysis was performed for at least 3 different polymer volume fractions. The theoretical predictions are discussed in the following section.

Results

We present the results for diameter ratios of 6:5:1, 7:5:1, 8:5:1 and 9:5:1 (protein 1:protein 2:polymer) in Tables 1-4, each of which shows the total coexistence volume fraction of protein in the fluid phase corresponding to the *two* intersection points shown in Figure 1b (when both exist). We have performed this determination for x_1 values of 0.0, 0.05, 0.10, 0.30, 0.50, 0.70, 0.90, 0.95, and 1.0, and for ϕ_3 values of 0.0, 0.01, 0.02, 0.04, 0.05, 0.10, 0.20 and 0.30. The total coexistence volume fraction in the fluid phase at which precipitation occurs

Table 1. Total Coexistence Volume Fractions for Proteins 1 and 2 as a Function of Polymer Concentration and Protein Mole Fraction for a Diameter Ratio = 6:5:1

	Polymer Volume Fractions, ϕ_3									
	0.00		0.05		0.10		0.20		0.30	
x_1	Prot 1	Prot 2	Prot 1	Prot 2	Prot 1	Prot 2	Prot 1	Prot 2	Prot 1	Prot 2
0.00	—	**0.497**	—	**0.501**	—	**0.495**	—	**0.415**	—	**0.0457**
0.05	0.584	**0.507**	0.544	**0.485**	0.494	**0.449**	0.343	**0.295**	0.0735	**0.045**
0.10	0.562	**0.517**	0.522	**0.495**	0.472	**0.459**	0.311	**0.305**	**0.0456**	0.0489
0.15	0.553	**0.529**	0.511	**0.505**	**0.461**	0.468	**0.295**	0.315	**0.0364**	0.0524
0.20	0.544	**0.537**	**0.504**	0.514	**0.453**	0.478	**0.280**	0.326	**0.0276**	0.0564
0.30	**0.533**	0.554	**0.495**	0.533	**0.445**	0.497	**0.264**	0.348	**0.0204**	0.0665
0.50	**0.521**	0.588	**0.487**	0.569	**0.438**	0.537	**0.246**	0.397	**0.0144**	0.0944
0.70	**0.511**	0.623	**0.482**	0.609	**0.436**	0.583	**0.237**	0.461	**0.0117**	0.144
0.90	**0.501**	0.677	**0.479**	0.674	**0.437**	0.662	**0.231**	0.579	**0.0096**	0.277
0.95	**0.499**	0.706	**0.478**	0.717	**0.437**	0.711	**0.268**	0.653	**0.0096**	0.373
1.00	**0.497**	—	**0.503**	—	**0.495**	—	**0.319**	—	**0.0097**	—

Boldfaced numbers = protein precipitating at the given polymer volume fraction and protein mole fraction
— = no intersection of the μ_i/kT vs. p/kT curves

Table 2. Total Coexistence Volume Fractions of Proteins 1 and 2 as a Function of Polymer Concentration and Protein Mole Fraction for a Diameter Ratio = 7:5:1

	Polymer Volume Fractions, ϕ_3					
	0.00		0.05		0.10	
x_1	Prot 1	Prot 2	Prot 1	Prot 2	Prot 1	Prot 2
0.00	—	**0.497**	—	**0.501**	—	**0.495**
0.05	**0.516**	0.518	**0.469**	0.493	**0.412**	0.456
0.10	**0.505**	0.537	**0.459**	0.512	**0.401**	0.474
0.30	**0.503**	0.594	**0.460**	0.573	**0.401**	0.539
0.50	**0.507**	0.633	**0.469**	0.621	**0.411**	0.595
0.70	**0.506**	0.665	**0.475**	0.664	**0.420**	0.652
0.90	**0.500**	0.706	**0.477**	0.728	**0.428**	—
0.95	**0.498**	0.731	**0.483**	—	**0.429**	—
1.00	**0.497**	—	**0.494**	—	**0.490**	—

Boldfaced numbers = lower values.

is the *lower* value. These tables indicate which of the two proteins precipitates and the total protein volume fraction at which this precipitation occurs. Note that in all the cases examined, the diameter ratio between the smaller protein and the polymer is kept constant (ratio = 5.0).

In this section, we examine the influence on protein solubility of the diameter ratio between the two proteins, the mole fraction in the mixture (type of mixture), and the concentration of the polymer added. We are interested particularly in learning how variations in these parameters determine which protein precipitates. Since the solubility is linearly related to the coexistence volume fraction (from Eq. 12), we will speak of them interchangeably in our discussion of these phase diagrams. Figures 4a, 4b and 4c show phase diagrams plotted as total coexistence volume fraction of protein vs. the polymer volume fraction added, at protein 1 mole fraction of 0.50, 0.10 and 0.05, respectively. The diameter ratio of protein 1: protein 2: polymer is 6:5:1.

Figure 4a represents the most typical phase diagram found for these systems in that the precipitate is always the larger protein, protein 1. Shown here is a plot of ϕ^{coex}, the total protein volume fraction when the fluid and solid phases are in equilibrium vs. ϕ_3, the volume fraction of polymer added for diameter ratio of 6:5:1 and $x_1 = 0.50$. The "solubility curve" for a species 1 protein (labeled protein-1 solubility) is the lower curve in Figure 4a. This curve is not strictly the solubility curve for protein 1 (that would be ϕ_1^{coex} vs. ϕ_3), but is related to it in a simple manner by:

$$\phi_1^{coex} = \phi^{coex} - \phi_2 \tag{13}$$

Below and to the left of this curve, there is a fluid regime (labeled fluid). At any point in this region, not enough polymer has been added to elicit either protein out of solution. The area between the solubility curve for protein 1 and the solid-phase curve (labeled fluid-solid 1) is a regime where there is an equilibrium between the fluid and a solid (precipitate) phase

Table 3. Total Coexistence Volume Fractions of Proteins 1 and 2 as a Function of Polymer Concentration and Protein Mole Fraction for a Diameter Ratio = 8:5:1

	Polymer Volume Fractions, ϕ_3							
	0.00		0.02		0.04		0.08	
x_1	Prot 1	Prot 2	Prot 1	Prot 2	Prot 1	Prot 2	Prot 1	Prot 2
0.00	—	**0.497**	—	**0.499**	—	**0.500**	—	**0.496**
0.05	**0.457**	0.535	**0.441**	0.524	**0.421**	0.513	**0.376**	0.485
0.10	**0.457**	0.565	**0.442**	0.555	**0.422**	0.543	**0.377**	0.516
0.30	**0.482**	0.644	**0.469**	0.638	**0.449**	0.630	**0.403**	0.608
0.50	**0.499**	0.680	**0.488**	0.682	**0.470**	0.680	**0.426**	0.672
0.70	**0.504**	0.698	**0.496**	0.594	**0.481**	0.713	**0.441**	0.727
0.90	**0.498**	0.724	**0.495**	0.737	**0.484**	—	**0.450**	—
0.95	**0.495**	0.747	**0.493**	0.756	**0.483**	—	**0.452**	—
1.00	**0.497**	—	**0.498**	—	**0.487**	—	**0.475**	—

Boldfaced numbers = protein precipitating at the given polymer volume fraction and protein mole fraction
— = no intersection of the μ_i/kT vs. p/kT curves

Table 4. Total Coexistence Volume Fractions of Proteins 1 and 2 as a Function of Polymer Concentration and Protein Mole Fraction for a Diameter Ratio = 9:5:1

	Polymer Volume Fractions, ϕ_3							
	0.00		0.01		0.02		0.06	
x_1	Prot 1	Prot 2	Prot 1	Prot 2	Prot 1	Prot 2	Prot 1	Prot 2
0.00	—	**0.497**	—	**0.498**	—	**0.499**	—	**0.500**
0.05	**0.406**	0.556	**0.394**	0.545	**0.375**	0.533	**0.354**	0.519
0.10	**0.417**	0.602	**0.406**	0.591	**0.387**	0.579	**0.366**	0.565
0.30	**0.466**	0.709	**0.457**	0.704	**0.438**	0.696	**0.416**	0.688
0.50	**0.492**	0.731	**0.486**	0.740	**0.468**	0.750	**0.447**	0.757
0.70	**0.500**	0.843	**0.498**	0.743	**0.482**	0.760	**0.464**	—
0.90	**0.503**	0.849	**0.496**	0.753	**0.485**	0.585	**0.471**	—
0.95	**0.491**	0.858	**0.494**	0.766	**0.484**	0.792	**0.471**	—
1.00	**0.497**	—	**0.500**	—	**0.503**	—	**0.470**	—

Boldfaced numbers = protein precipitating at the given polymer volume fraction and protein mole fraction
— = no intersection of the μ_i/kT vs. p/kT curves

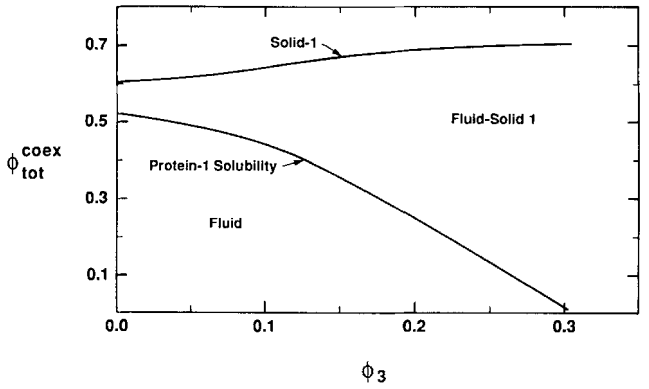

Figure 4a. Total coexistence volume fraction of protein vs. polymer volume fraction added: $x_1 = 0.50$ for protein 1:protein 2:polymer diameter ratios of 6:5:1.

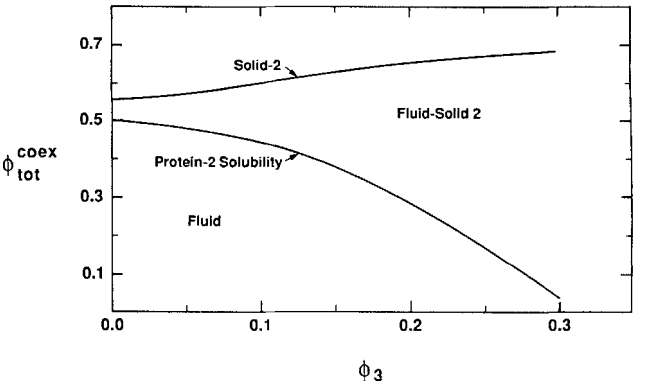

Figure 4c. Total coexistence volume fraction of protein vs. polymer volume fraction added: $x_1 = 0.05$ for protein 1:protein 2:polymer diameter ratios of 6:5:1.

of protein 1 of composition given by the curve labeled solid 1.

To understand this phase diagram it is helpful to consider the following example. If we begin adding polymer to a protein mixture at a total protein concentration of 0.30, there would be a fluid mixture of proteins and polymer (fluid) until the polymer volume fraction of 0.17 is reached. At this polymer volume fraction, protein 1 would start to precipitate. The fluid phase would be in equilibrium with a solid phase of protein 1 at a total protein volume fraction of 0.65. Any further increase in polymer concentration would increase the ratio of solid phase to the fluid phase within the two-phase region, labeled fluid-solid 1.

Figure 4b shows a phase diagram for a mixture which is rich in the smaller protein ($x_1 = 0.10$). This phase diagram shows the formation of a "eutectic" at a polymer concentration of 0.24. We find that the smaller protein precipitates at polymer concentrations less than 0.24, while the larger one precipitates at polymer concentrations greater than 0.24. At the "eutectic point," both proteins precipitate into their own solid phase and we obtain a mixed-solid phase of the same composition as the fluid mixture. At polymer concentrations below the eutectic point, the lower curve is the solubility curve for protein 2. In the region between this curve and the upper curve, there is a fluid-solid 2 equilibrium. At polymer concentrations greater than the eutectic, the lower curve is the solubility curve for protein 1, and the region between the two curves represents equilibrium between the fluid and a precipitate of protein 1 (fluid-solid 1).

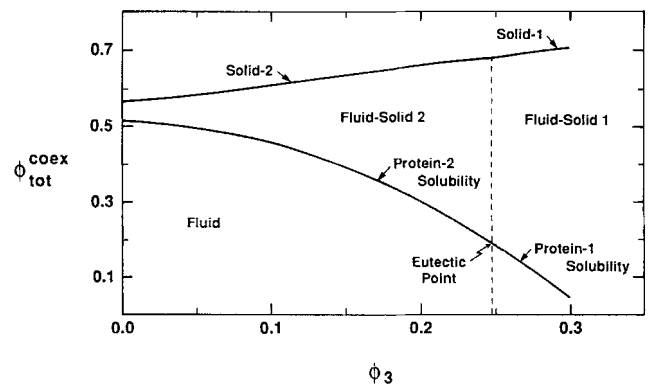

Figure 4b. Total coexistence volume fraction of protein vs. polymer volume fraction added: $x_1 = 0.10$ for protein 1:protein 2:polymer diameter ratios of 6:5:1.

Figure 4c is a phase diagram for a mixture even richer in the smaller protein ($x_1 = 0.05$). This figure is similar to Figure 4a, in that there is no eutectic formation except that it is protein 2 which precipitates at all polymer concentrations investigated. For a given total protein volume fraction, addition of polymer to a critical value precipitates protein 2 and we have an equilibrium between the fluid and a precipitate of protein 2, as illustrated in the fluid-solid 2 region.

The conclusions from the phase diagrams (Figures 4a–4c) and from Tables 1–4, can be summarized as follows.

(1) The theory predicts a preferential precipitation of the larger protein over the smaller one. We will refer to this tendency as the size effect. Exceptions to this rule occur only when the polymer concentration is very low and when the smaller protein is in large excess. For instance, Figure 4b shows that at all, but the highest, polymer concentrations, the more concentrated protein (protein 2) precipitates preferentially to the less concentrated (and in this case the larger) protein.

(2) Increasing the mole fraction of a particular protein in a mixture increases the likelihood that it will be the protein to precipitate. We will refer to this tendency as the concentration effect.

(3) Increasing the polymer concentration increases the likelihood that the larger protein will precipitate.

(4) At certain protein mole fractions, the theory predicts the formation of a eutectic at which both proteins precipitate into their own pure phases.

An alternative way to illustrate the phase behavior is to plot the total coexistence volume fraction, ϕ_{tot}^{coex}, vs. the protein mole fraction of the mixture, x_1, for various polymer volume fractions, ϕ_3. This is shown in Figure 5 (again for the 6:5:1 mixture) for polymer volume fractions of 0.0, 0.05, 0.10, 0.20 and 0.30. We know from our earlier discussion, that for each x_1 and polymer volume fraction value, only one of the two proteins precipitate, except at the eutectic shown in Figure 5 (dashed

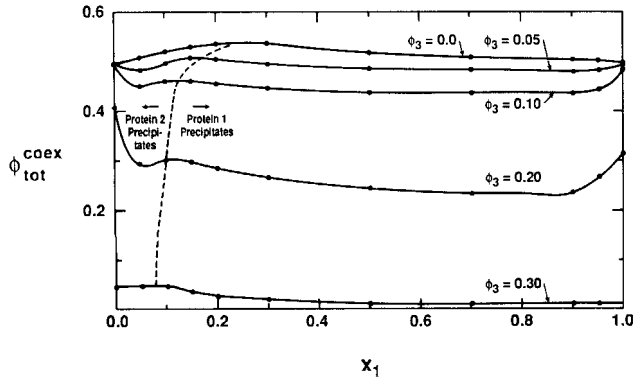

Figure 5. Total coexistence volume fraction of protein vs. protein 1 mole fraction for various polymer volume fractions for protein 1:protein 2:polymer diameter ratios of 6:5:1.

Points represent the mole fractions at which calculations were made; dashed line, locus of points at which precipitation shifts.

line). It shows the variation in the eutectic composition with polymer concentration, protein mole fraction, and total protein volume fraction. The dashed line is also the locus of points at which the precipitation shifts from precipitation of one protein to precipitation of the other. To its right, protein 1 precipitates, while to its left protein 2 precipitates. It is obvious that protein 1 precipitates at most x_1 values with the exceptions being at very low values of x_1. We note also the shift of this line to lower x_1 values with increasing polymer concentrations confirming the conclusion stated above that the addition of polymer also favors precipitation of the larger protein. Figure 5 clearly shows that addition of polymer reduces the solubility of both proteins as expected.

It is also of interest to explore the effect of the diameter ratio between proteins on their precipitation. Tables 2-4 show that as the diameter ratio between proteins is increased (6:5 to 9:5), precipitation of the larger protein occurs for more and eventually all x_1s and ϕ_3s. In other words, the "size effect" overwhelms the "concentration effect," even for mixtures very rich in the smaller protein. In fact, for every case that we studied, at x_1 values of 0.5 or greater, the larger protein always precipitates rather than the smaller one. Hence, we make the claim that size is the most important criterion in determining solubility behavior in these systems. This leads to the somewhat expected conclusion that the precipitation of the larger protein is further facilitated as the diameter ratio between proteins is increased. To reiterate, in our study we predict that the smaller protein precipitates *only* in the 6:5:1 and 7:5:1 cases and, within these subgroups, only for mixtures with $x_1 < 0.30$.

We offer the following physical explanation for our findings. It is known that protein solubility decreases with polymer addition. The theory explains this reduction in terms of an increase in the excluded-volume attraction between protein molecules due to the presence of the polymer. This attraction is known to increase with the diameter ratio between protein and polymer. Thus, if we have two proteins, one of which is larger, addition of polymer would increase the attraction between the larger proteins more than between smaller ones. Hence, an increase in polymer concentration further favors precipitation of protein 1. This explains the shift from precipitation of protein 2 to that of protein 1 with an increase in polymer concentrations for mixtures exhibiting the eutectic-type behavior.

Table 5. Coexistence Volume Fraction of Protein 1 for a Diameter Ratio = 6:5:1

	Polymer Volume Fractions, ϕ_3				
x_1	0.00	0.05	0.10	0.20	0.30
0.10	—	—	—	—	0.0073
0.30	0.227	0.211	0.189	0.112	0.0087
0.50	0.330	0.309	0.277	0.156	0.0091
0.70	0.409	0.386	0.349	0.190	0.0094
0.90	0.471	0.450	0.410	0.217	0.0091
0.95	0.484	0.464	0.424	0.231	0.0093
1.00	0.497	0.503	0.495	0.319	0.0097

So far we have been discussing exclusively the behavior of the total coexistence volume fraction. Since we would like to predict the actual solubilities of protein in protein mixtures, it is worthwhile to examine the *individual* coexistence volume fractions of the precipitating protein. This quantity is related directly to the solubility (Eq. 12). In Table 5 we list the coexistence volume fractions of protein 1 for the 6:5:1 case. These are calculated from the total coexistence values in Table 1 using Eq. 13. In Figure 6, the coexistence volume fraction of protein 1 is plotted vs. polymer volume fraction for various protein mixtures. This figure is for a diameter ratio of 6:5:1. The following conclusions can be drawn from this figure. First, the solubility decreases with addition of polymer, as expected. Second, the "intrinsic" solubility or the solubility in the absence of the polymer of protein 1 depends on the mole fraction of the mixture. Hence, even in this simple model, where any associative/repulsive behavior between the two proteins is ignored (no biological intricacies—only variation is size), the presence of one affects the solubility of the other in the absence of the polymer. Third, it is rather interesting to note from such a plot that the addition of the smaller protein reduces the solubility of the larger one.

Since experimental data are usually presented in the form of solubility curves relating log (solubility) to % polymer (wt./vol.), it is instructive to report the theoretical predictions too in terms of these quantities. We use Eq. 12 to calculate

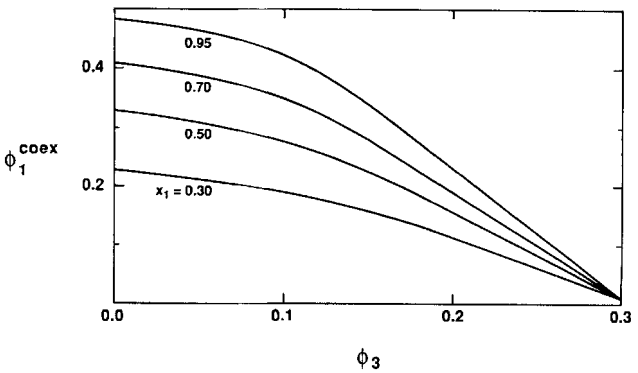

Figure 6. Coexistence volume fraction of protein 1 vs. polymer volume fraction for various protein mole fractions for protein 1:protein 2:polymer diameter ratios of 6:5:1.

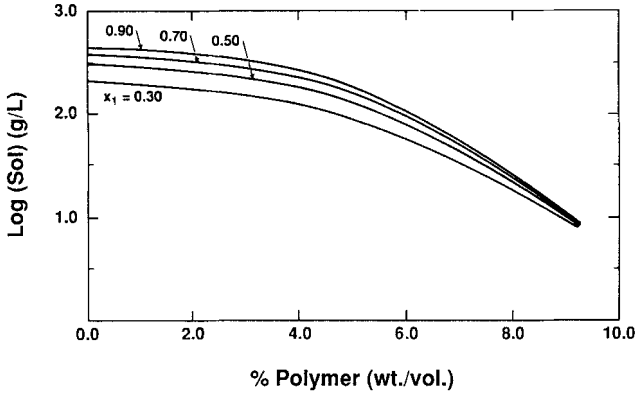

Figure 7. Log(solubility) of protein 1 (g/L) vs. %polymer (wt./vol.) for protein 1:protein 2:polymer diameter ratios of 6:5:1 for a variety of protein 1 mol. fractions.

the solubilities of the precipitating protein with representative values of 0.72 for $\overline{V}_2$ and $\overline{V}_3$ and 0.35 for δ_1. We calculate the solubility of protein 1 for the 6:5:1 case in Figure 7 for a variety of protein compositions. We have noted in our earlier article that the linearity in these curves does not extend to zero polymer concentration. We see a similar behavior for all the protein mixtures plotted in this figure. Figure 7 shows that at high polymer concentrations (or in the linear, experimentally significant part of the curve), all the curves tend to come together. This implies that at high polymer concentrations the effect of the second protein on the solubility of the larger one is negligible.

Discussion and Comparison with Experiment

A consequence of the model's restriction to pure precipitates is that we can have two different solid phases in equilibrium with the fluid phase *only* at a single mole fraction of protein (Figures 2 and 3). At any point other than the eutectic, the second protein can precipitate after the first one but only when the proteins in the fluid phase have disappeared. The question arises then, do real protein 1/protein 2/polymer/water systems exhibit such behavior? The answer is no. In many experimental systems, it is indeed possible to have the proteins present in the fluid phase and in equilibrium with two (or more) different proteins in the solid phase over a *range* of protein or polymer concentrations. A possible explanation why the theory is unable to predict this type of equilibrium may have to do with our assumption of pure precipitates. We have treated the precipitation of proteins from protein mixtures as if each protein can precipitate only into its own phase and thus we require *three* phases to be in equilibrium when the fluid and both precipitates exist together. If we were able to model a mixed solid phase (single phase), then the Gibbs phase rule would allow for the precipitation of *both* proteins into the same phase over a range of protein or polymer concentrations.

The question that must be raised then concerns the nature of the solid (precipitate) phase (or phases) on a microscopic level. Does a precipitate containing two proteins represent two phases, or are the two proteins in one phase, say forming, a solid solution? At the moment it is not clear whether most protein mixtures precipitate into a single solid phase (pure or mixed phase) or into more than one phase each containing pure protein. The evidence in the literature on precipitation of protein mixtures indicates that the structure of the solid phase or phases depends on the specifics of the protein mixture. A study by Haire (1984) on the precipitation of hemoglobin suggests that extensive coprecipitation of two forms of hemoglobin does in fact occur and a mixed solid phase is formed. In other words, they see a form of "comingling" (formation of solid solutions) on a molecular level. In contrast, the experiments of Polson et al. (1964) who precipitated a mixture of plasma proteins by PEG found that both pure protein and multiple protein precipitation depend on the concentration of protein and polymer. Further, their experiments implied that when there was a mixture of precipitates in the solid phase, the mixing is only on a macroscopic level, thereby implying the existence of two (or more) precipitate phases in equilibrium with the fluid. It is known that a particular protein, which by itself will not precipitate, will be carried into the precipitate by a second precipitating protein (Foster, 1973; Kula, 1991). What remains unclear is: whether the "included" protein remains an impurity within the crystal lattice of the precipitating protein (in which case there really is only one solid phase—the precipitating protein); whether it remains in the mother liquor associated with crystal formation (a second phase); or whether it too forms its own solid phase. It appears therefore that the microscopic structure of the precipitate is a function of the specific proteins involved in the precipitation leaving the overall picture unclear at the present time (Ingham, 1990; Kula, 1991). Therefore, while the ability to model a mixed solid phase will allow the theory of predict equilibrium between the fluid and more than one precipitate over a range of protein or polymer concentrations, we are not sure if that would indeed be the appropriate refinement to the theory.

To understand the nature of the solid phase better, we performed a few experiments using PEG to precipitate a mixture of two different colored proteins: catalase (green) and BSA (white). Our aim in performing these experiments was not to obtain quantitative results for the solubility, but simply to obtain visual evidence of the nature of the precipitate. We found by visual inspection that the precipitate ranged from what appeared to be relatively pure catalase (green precipitate—no white flakes of BSA) to an intermingling of green and white (on a macroscopic level) depending on the relative amounts of catalase and BSA. Under no circumstances did we see a purely white precipitate. Catalase (MW $\approx$ 250,000) is much larger than BSA (MW $\approx$ 65,000) and therefore is expected to be preferentially precipitated by PEG. We did not perform microscopic analysis to determine if there was any mixing on a molecular level in our experiments. However, the preferential precipitation of catalase (the larger protein) over BSA is to verify our claim that size is the most important criterion in protein precipitation by nonionic polymer.

We are unaware of systematic experiments on the addition of PEG to protein mixtures which explore the effect of protein size on solubility. However, the experiments of Polson et al. (1964) seem to be in accord with our predictions. In their experiments, Polson et al. fractionated plasma protein using PEG and found that fibrinogen precipitated at the lowest polymer concentrations, followed by the γ-globulins, β-globulins, and then albumin. These observations can be predicted by the theory by noting that the size order is fibrinogen > γ-globulin > β-globulin > albumin. This order of precipitation serves

to confirm our prediction that size is the most important consideration in precipitation of protein mixtures.

Development of Theory: Electrostatic Effects

We have considered the variation of protein solubility in binary protein mixtures with the size and concentration of both proteins and the polymer, particularly focusing on the order of precipitation of the proteins in these systems. We now turn our attention to the effect of charge on the solubility of binary mixtures of proteins in the presence of nonionic polymer and extend our treatment to include the effects of electrostatic interactions. We study the effect of the variation of protein charge (related to pH) and ionic strength on the precipitation of protein mixtures. The theory is developed by employing the same fundamental approach as in the first part of this article. The two main additions are the inclusion of the effect of protein charge and added salt on the solubility behavior of the two proteins. The earlier results, therefore, are a special case of this study, since there the charge on both proteins was zero and no additional salt was added.

We calculate the electrostatic contribution to the chemical potential using an analytic solution of the mean spherical approximation which is applicable to a mixture of charged hard spheres (Blum, 1975). Although our primary aim is to examine the effect of electrostatic parameters on solubility, the MSA also accounts for the finite size of the ions (unlike the Debye-Hückel theory it accounts for core exclusion effects). Thus, we can calculate the effect of solubility of both the protein charge and protein size, and examine their relative importance. Our goal is to examine how the changes in the protein charges determine which of the two proteins precipitates. In this section, we consider a diameter ratio of 6:5:1. Keeping the two proteins at fairly equal sizes minimizes the contribution of the size effect (which is the primary driving force in the precipitation of proteins by polymer) and allows us to compare it with our earlier results when this particular size ratio (6:5:1) was extensively studied. It would be straightforward to apply this technique to other diameter ratios.

Molecular model

The system we consider here is a binary liquid mixture of proteins (species 1 and 2), polymer (species 3) the protein's counterions (species 4 and 5) and salt anions and cations (species 6 and 7). The salt has been added to allow us to study the effect on solubility of ionic strength. The fluid phase is aqueous and the solvent is treated as a continuum. Hence, we do not explicitly take into account the water but rather treat it as a background fluid. As before, we employ the convention that species 1 is the larger protein. This seven-component system is in equilibrium with an aqueous precipitate of protein 1 or 2. We model the two protein molecules as charged hard spheres of diameter and charge, d_1,z_1 and d_2,z_2, respectively. The counterions and the added salt (if any) are also modeled as charged hard spheres of diameters and charges d_i and z_i, $i=4$ to 7. The polymer molecules are modeled as spheres of diameter d_3, which are hard with respect to all species but which can freely penetrate each other. As was done previously, the effect of the added polymer is included via an excluded-volume attraction felt by the protein molecules due to the presence of the polymer solution.

The mechanism by which the volume-exclusion attraction between proteins in polymer solution arises has been explained earlier. In this section, we are decoupling, in a sense, the effect of the polymer solution on the solubility behavior of the two proteins from the net effect of other species. The polymer is assumed to contribute only to the intermolecular potential (actually potential of mean force) between the two proteins via this volume exclusion attraction. The polymer does not create an excluded-volume interaction between ions or between protein and ions. Hence, the forms for the attractive intermolecular potential between protein molecules due to the presence of polymer, $u_{ij}^{vex}(r)$, are identical to that described earlier in Eqs. 1 and 2.

As mentioned before, the micro-ions do not feel the effect of polymer, and therefore the volume exclusion potential for all other species ($i,j=4$ to 7) reduces to the hard-core interaction:

$$u_{ij}^{hc}(r)=\begin{cases}\infty, & r<d_i\\ 0, & r\geq d_i\end{cases} \tag{14}$$

In addition to the volume exclusion potential, the charges on the proteins and on all the micro-ions lead to an electrostatic interaction between all the charged species. This interaction is taken to be the Coulomb potential. Hence, between *all charged species* (i,j) the electrostatic interaction is given by:

$$u_{ij}^{elec}(r)=\frac{e^2z_iz_j}{\epsilon_0 r} \tag{15}$$

where e is the elementary charge and ϵ_0 is the dielectric constant of the continuum.

In summary, the total intermolecular potentials of various species are given by:

$$u_{ij}(r)=u_{ij}^{vex}(r)+u_{ij}^{elec}(r)\ \text{(protein-protein)} \tag{16}$$

$$u_{ij}(r)=u_{ij}^{hc}(r)+u_{ij}^{elec}(r)\ \text{(protein-ion,ion-ion)} \tag{17}$$

In Eqs. 16 and 17, various intermolecular potentials are obtained as appropriate from Eqs. 1, 2, ?? and 15.

The chemical potential of this system is calculated by combining the MSA, which treats the electrostatic part of the potential, and perturbation theory, which treats the volume exclusion potential between proteins and the hard core potential between proteins and ions and between ions. The MSA *directly* provides the excess chemical potential (over a hard-sphere mixture state) due to the charges on all species. The chemical potential of all species is therefore given by:

$$\mu_i=\mu_i^{MSA}+\mu_i^{pert}\quad (i=1,\ 2,\ 4\ \text{to}7) \tag{18}$$

The first term on the righthand side of Eq. 18 is the excess chemical potential (over a hard-sphere mixture state) of species i due to the charges on all species (electrostatic contribution). This term is obtained directly from the solution of the MSA for a six-component mixture of charged hard spheres (the proteins, counterions, and salt anions and cations). The second term includes both the volume exclusion and the hard-core potentials. The second term is evaluated using the perturbation theory where the reference state is chosen to be a hard-sphere mixture.

In the evaluation of the second term in Eq. 18, we neglect its contribution to the chemical potential associated with the hard-core interactions between proteins and ions and between ions. Even though we are treating a six-component system, the reference system is taken to be a *binary* hard-sphere mixture of proteins. The justification for this approximation is that the error in $\mu^{hs}_{protein}$ (or $\mu^{ref}_{i=1,2}$) due to the finite size of the ions in the hard-sphere reference state is quite small, because $\mu^{hs}_{protein}$ depends on the volume fraction of various species and not on the number density. We have chosen to make this approximation, because the Percus-Yevick (PY) and the PY-based approximations are highly inaccurate for asymmetric mixtures of hard spheres (Fries and Hansen, 1983; Ballone et al., 1986). In particular, the PY approximation fails for dilute solutions of big spheres in a solution of smaller ones, which exactly corresponds to the situation we are considering. We are therefore unable to include a higher number of components in the reference state. Such an approximation would be less justifiable if we were interested in the partitioning behavior (between fluid and solid phases) of the counterions.

Mean spherical approximation

An important relationship in statistical mechanics is the Ornstein-Zernike (O-Z) equation which can be considered to be the defining equation for the direct correlation function $c(r)$. The O-Z equation relates the pair correlation function $g(r)$ to the direct correlation function. To solve for $c(r)$ and $g(r)$ it is necessary to obtain a second relationship, called the closure, between these two functions. Many such closures have been proposed, one of which is the mean spherical approximation. An important advantage of the MSA is that it can be solved analytically for certain potentials. The MSA has been used to calculate the mean ionic activity coefficients of ionic species in aqueous electrolyte mixtures, and the agreement with experimental data has been shown to be quite good (Triolo et al., 1976; Vericat and Grigera, 1982).

The Ornstein-Zernike equation:

$$h_{ij}(r) = c_{ij}(r) + \rho \int_0^\infty c_{ik}(r) h_{jk}(r) dr_k \tag{19}$$

states that the total correlation function $h(r_{ij}) \equiv [g(r_{ij}) - 1]$ is divided into a direct correlation function, $c(r_{ij})$, and an indirect part which is given by the convolution. The convolution accounts for the effect that particle i has on particle j through a third particle k, directly or indirectly. Within the MSA, the following closure is employed:

$$g_{ij}(r) = 0 \qquad r \le d_{ij}$$

$$c_{ij}(r) = \frac{u_{ij}(r)}{kT} \qquad r > d_{ij} \tag{20}$$

where $d_{ij} = (d_i + d_j)/2$. Blum (1975) and Blum and Hoye (1978) have obtained the solution to the MSA for a multicomponent mixture of charged hard spheres of arbitrary size and charge. This solution has been used by various investigators to evaluate the individual ionic activity coefficients γ_i of electrolytes (Triolo et al., 1976; Vericat and Grigera, 1982). The logarithm of the ionic activity coefficient is identical to the reduced excess chemical potential over a hard-sphere mixture reference state, μ_i^{ex}/kT. Blum and independently Hiroike (1977) have obtained the excess (over the hard-sphere mixture reference state) free energy due to the charges using the MSA analysis. The activity coefficient for a mixture of charged hard spheres of size d_i, and charge z_i, $i = 1, n$ can be calculated from:

$$\ln \gamma_i = \beta \mu_i^{ex} = \beta \Delta E + S_i \tag{21}$$

where ΔE is the excess internal energy per unit volume due to the charges and S_i is a function of the universal scaling parameter Γ. This parameter, Γ, in turn depends on the size d_i, charge z_i and density ρ_i of the various species. Γ can be shown to be analogous to the inverse screening length κ within the Debye-Hückel theory; in the infinite dilution limit, 2Γ goes to the Debye inverse length.

The excess chemical potential over a hard-sphere mixture reference state can be obtained using Eq. 21 by evaluating ΔE and S_i from:

$$\frac{\epsilon_0 \Delta E}{e^2} = -\left[\Gamma \sum_{i=1}^{n} \left(\frac{\rho_i z_i^2}{1 + \Gamma d_i} \right) + \frac{\pi}{2\delta} \Omega P_n^2 \right] \tag{22}$$

$$S_i = -P_n d_i \left(\Gamma a_i + \frac{\pi}{12\Delta} \alpha^2 P_n d_i^2 \right) \Big/ 4\Delta \tag{23}$$

where ϵ_0 is the dielectric constant of the pure solvent and e is the charge on an electron.

In the solution of the MSA for charged hard spheres, expressions for the thermodynamic properties such as the excess internal energy (Eq. 22) are written as the sum of two terms: one which is exactly in the Debye-Hückel form, but with 2Γ as the shielding parameter (instead of κ), and the other contains the parameter P_n. This parameter P_n is also a function of the scaling parameter Γ which is calculated using the following equations:

$$\Delta = 1 - \frac{\pi}{6} \sum_{i=1}^{n} \rho_i d_i^3 \tag{24}$$

$$P_n = \frac{1}{\Omega} \sum_{i=1}^{n} \left(\frac{\rho_i d_i z_i}{1 + \Gamma d_i} \right) \tag{25}$$

$$\alpha^2 = \frac{4\pi e^2}{\epsilon_0 kT} \tag{26}$$

$$\Omega = 1 + \frac{\pi}{\Delta} \sum_{i=1}^{n} \left(\frac{\rho_i d_i^3}{1 + \Gamma d_i} \right) \tag{27}$$

The universal parameter Γ is given by:

$$2\Gamma = \alpha \left\{ \sum_{i=1}^{n} \rho_i \left[\frac{z_i - (\pi/2\Delta) d_i^2 P_n}{1 + \Gamma d_i} \right]^2 \right\}^{1/2} \tag{28}$$

The set of Eqs. 24–28 are solved iteratively using the size, charge and concentration of the various species as input parameters. We used the secant method to solve the one-variable equation $f(\Gamma) = 0$ (from Eq. 28) (Burden et al., 1981). Given

the input parameters and two initial guesses for Γ (a good starting guess is the Debye length κ—we used two values bracketing κ), the various parameters in Eqs. 24-27 are calculated and the resulting parameters Δ, P_n, and Ω are substituted into Eq. 28 to obtain a new value for Γ using the secant method. This process is repeated until convergence is achieved. We thus obtain the universal scaling parameter Γ and hence $\beta\mu_i^{ex}$.

Determination of phase transition

To predict phase transitions it is necessary to perform the calculations for both a fluid phase and a solid (precipitate) phase. In the fluid phase we have a mixture of proteins; however, the solid phase is assumed to be pure. In other words, we do not allow for a solid-phase mixture (coprecipitation); each protein is assumed to precipitate into its own solid phase. We assume that the micro-ions do not enter the solid phase, since in experimental studies of protein precipitation, free micro-ions are not found in the precipitate. The precipitated protein is neutral in the solid phase, and we ignore the slight change in size of the protein due to the "attachment" of these ions to the protein. We have invoked the principles of McMillan and Mayer (see Mahadevan and Hall, 1990) in treating the protein:protein:polymer system as a pseudo two-component system. Implicit in this approach is the fact that the concentration of the polymer molecules around the protein is equal in all phases. Hence, the polymer is present in the solid phase. The solid-phase free energies are calculated in an identical manner to that described in Mahadevan and Hall (1990). The free energies are calculated for one mixed fluid phase and *two* solid phases (protein 1 and protein 2), and a thermodynamic stability analysis is performed to decide which of the two species is actually at its solubility limit at the given conditions. The implications of the neglect of a mixed solid phase in this analysis have been discussed before.

The system (two proteins, associated counterions, and salt anions and cations) is completely defined when the diameter ratios of the two proteins to the polymer, (d_1/d_3 and d_2/d_3), the charges on both proteins, the diameter ratios of the counterions, the diameter ratios of the added salt to the polymer, d_i/d_3, $i=4$ to 7, the mole fraction, x_1, of one of the proteins in the fluid phase, the volume fraction, $\phi_3=(\pi n_3 d_3^3)/6$, of the polymer added to the fluid, and the total volume fraction $\phi_{total}=\phi_1+\phi_2$ of proteins in the solution are specified. For a given set of molecular parameters and thermodynamic variables, the fluid-phase chemical potentials and pressure are determined numerically using Eqs. 18 and 7. The solid-phase variables are calculated in a manner identical to that described by ref. 11.

A thermodynamic stability analysis is performed on the protein mixture system to determine the conditions at which precipitation occurs. In the fluid phase, the chemical potentials of both species are calculated at discrete values of the total volume fraction of protein, ϕ, using Eq. 18. In the solid phase, the chemical potential of each protein is calculated for varying values of the individual volume fraction of each protein [$\phi_1=(\pi\rho_1 d_1^3)/6$ and $\phi_2=(\pi\rho_2 d_2^3)/6$]. Here, ρ_i is the number density of species i. Next, the chemical potentials of each species in the fluid and the two pure solid phases are plotted vs. the reduced pressure.

The equilibrium between fluid and solid is determined in a manner identical to that used previously. The calculations were performed for a diameter ratio of 6:5:1 (protein 1:protein 2:polymer). Protein 1 was always taken to be the larger protein. The charge on both proteins was varied. The following pairs of charges on the proteins were considered: $(z_1,z_2)=(0,10)$, (5,0), (5,5), (10,0), and (−5,0). For each pair of protein charges, 5 different protein mole fraction mixtures were studied ($x_1=0.10$, 0.30, 0.50, 0.70, and 0.90) for 4 different polymer volume fractions ($\phi_3=0.0$, 0.10, 0.20, and 0.30) and two salt concentrations (0.0 and 0.30 M). In all the cases studied, the charges of the micro-ions were set equal to 1. The following diameters were used for the various species: $d_1=120$, $d_2=100$, $d_3=20$, $d_4=2.5$, $d_5=2.0$, $d_6=3.0$, and $d_7=3.6$ (All diameters are in Angstroms). The diameters were chosen to correspond to globular protein molecular weights between 80,000 and 160,000 daltons (d_1 and d_2) with counterions of H^+ and OH^- (d_4 and d_5); the salt added was assumed to be NaCl (d_6 and d_7). Ionic diameters for NaCl were obtained from Triolo et al. (1976). The polymer diameter corresponds to polyethylene glycol molecules with an approximate molecular weight of 2,000 daltons. By varying the salt concentration we were, in essence, changing the ionic strength of the solution since $I=(1/2)\sum_i z_i^2 M_i$. The molar salt concentrations was converted to number densities (in particles/Angstrom^3) for use in Eqs. 21-22 by:

$$\rho_i=\rho\nu_i=6.0225\times10^{-4}\,\mathrm{M} \tag{29}$$

where ν_i is the stoichiometric coefficient in the electrolyte dissociation reaction, and M is the molar concentration of the salt (Triolo et al., 1976).

Table 6. Coexistence Volume Fractions of Total Protein for Precipitation of Protein 1 and 2 as a Function of Protein Mole Fraction and Polymer Volume Fraction for $z_1=10$ and $z_2=0$

	$\phi_3=0.0$				$\phi_3=0.10$				$\phi_3=0.20$				$\phi_3=0.30$			
	$C_{salt}=0$		$C_{salt}=0.3$ M		$C_{salt}=0$		$C_{salt}=0.3$ M		$C_{salt}=0$		$C_{salt}=0.3$ M		$C_{salt}=0$		$C_{salt}=0.3$ M	
x_1	pr1	pr2	pr1	pr2	pr1	pr2	pr1	pr2	pr1	pr2	pr1	pr2	pr1	pr2	pr1	pr2
0.10	—	**0.517**	—	**0.518**	0.614	**0.458**	0.631	**0.460**	0.483	**0.305**	0.497	**0.306**	0.209	**0.048**	0.232	**0.048**
0.30	—	**0.553**	—	**0.555**	0.647	**0.495**	0.660	**0.495**	0.510	**0.347**	0.524	**0.348**	0.209	**0.066**	0.233	**0.067**
0.50	—	**0.585**	—	**0.584**	0.692	**0.534**	0.708	**0.537**	0.544	**0.395**	0.570	**0.396**	0.225	**0.094**	0.241	**0.096**
0.70	—	**0.621**	—	**0.623**	0.710	**0.583**	0.727	**0.584**	0.584	**0.456**	0.603	**0.456**	0.243	**0.143**	0.260	**0.146**
0.90	—	**0.673**	—	**0.672**	0.734	**0.662**	0.751	**0.662**	0.626	**0.571**	0.650	**0.573**	**0.268**	0.27	**0.260**	0.273

Boldfaced numbers = protein precipitating at the given protein charges, protein mole fraction and polymer volume fraction
— = no intersection of the μ_i/kT vs. p/kT curves

Table 7. Coexistence Volume Fractions of Total Protein for Precipitation of Protein 1 and 2 as a Function of Protein Mole Fraction and Polymer Volume Fraction for $z_1 = 5$ and $z_2 = 0$

	$\phi_3 = 0.0$				$\phi_3 = 0.10$				$\phi_3 = 0.20$				$\phi_3 = 0.30$			
	$C_{salt} = 0$		$C_{salt} = 0.3$ M		$C_{salt} = 0$		$C_{salt} = 0.3$ M		$C_{salt} = 0$		$C_{salt} = 0.3$ M		$C_{salt} = 0$		$C_{salt} = 0.3$ M	
x_1	pr1	pr2	pr1	pr2	pr1	pr2	pr1	pr2	pr1	pr2	pr1	pr2	pr1	pr2	pr1	pr2
0.10	0.596	**0.517**	0.615	**0.521**	0.503	**0.458**	0.523	**0.461**	0.348	**0.305**	0.38	**0.307**	0.06	**0.05**	0.063	**0.052**
0.30	0.586	**0.554**	0.592	**0.556**	**0.493**	0.496	0.502	**0.499**	**0.323**	0.347	**0.343**	0.350	**0.029**	0.066	**0.058**	0.066
0.50	0.588	**0.587**	**0.587**	0.590	**0.499**	0.535	**0.499**	0.537	**0.319**	0.396	**0.331**	0.399	**0.021**	0.093	**0.043**	0.095
0.70	**0.593**	0.622	**0.584**	0.625	**0.507**	0.580	**0.501**	0.584	**0.321**	0.458	**0.327**	0.462	**0.016**	0.144	**0.036**	0.145
0.90	**0.596**	0.674	**0.581**	0.678	**0.516**	0.658	**0.505**	0.657	**0.326**	0.573	**0.326**	0.581	**0.014**	0.274	**0.031**	0.278

Boldfaced numbers = protein precipitating at the given protein charges, protein mole fraction and polymer volume fraction.

Table 8. Coexistence Volume Fractions of Total Protein for Precipitation of Protein 1 and 2 as a Function of Protein Mole Fraction and Polymer Volume Fraction for $z_1 = -5$ and $z_2 = 0$

	$\phi_3 = 0.0$				$\phi_3 = 0.10$				$\phi_3 = 0.20$				$\phi_3 = 0.30$			
	$C_{salt} = 0$		$C_{salt} = 0.3$ M		$C_{salt} = 0$		$C_{salt} = 0.3$ M		$C_{salt} = 0$		$C_{salt} = 0.3$ M		$C_{salt} = 0$		$C_{salt} = 0.3$ M	
x_1	pr1	pr2	pr1	pr2	pr1	pr2	pr1	pr2	pr1	pr2	pr1	pr2	pr1	pr2	pr1	pr2
0.10	0.595	**0.517**	0.629	**0.522**	0.503	**0.458**	0.535	**0.461**	0.348	**0.305**	0.393	**0.307**	0.06	**0.048**	0.068	**0.052**
0.30	0.585	**0.553**	0.609	**0.559**	**0.493**	0.496	0.517	**0.500**	**0.332**	0.347	**0.346**	0.350	**0.028**	0.062	**0.061**	0.066
0.50	0.588	**0.587**	0.606	**0.594**	**0.498**	0.535	**0.516**	0.541	**0.319**	0.396	**0.335**	0.399	**0.022**	0.094	**0.045**	0.094
0.70	**0.592**	0.622	**0.6057**	0.629	**0.507**	0.580	**0.52**	0.588	**0.321**	0.458	**0.334**	0.462	**0.016**	0.144	**0.037**	0.145
0.90	**0.595**	0.674	**0.605**	0.683	**0.516**	0.659	**0.526**	0.671	**0.325**	0.574	**0.330**	0.581	**0.014**	0.274	**0.031**	0.276

Boldfaced numbers = protein precipitating for the particular set of protein charges, mole fraction and polymer volume fraction.

Results and Discussion

We present the results for the diameter ratio of 6:5:1 (protein 1:protein 2:polymer) in Tables 6–10, each of which shows the total coexistence volume fraction ϕ_{tot}^{coex} of protein in the fluid phase (volume fraction of total protein at which precipitation occurs) corresponding to the intersection of the μ_i/kT vs. p/kT curve for each species i. The lower value of the two numbers, which is in boldface, corresponds to the protein that actually precipitates for that particular set of protein charges, mole fraction and polymer volume fraction. Blank spaces indicate that there was no intersection of the μ_i/kT vs. p/kT curves for that particular protein. Each table is for a given set of protein charges. Within each table, we include the results for every protein mixture studied and for all the polymer volume fractions examined for that particular set of charged proteins. In addition, each table includes results for both values of the salt concentration. Note that in all the cases examined, the diameter ratio between the proteins and the polymer is kept constant. These tables indicate which of the two proteins precipitates and the total protein volume fraction at which this precipitation occurs.

Recall that the solubility of a protein is linearly related to the coexistence volume fraction of that particular protein ϕ_i^{coex}:

$$\text{Sol} = \frac{1{,}000\phi_i^{coex}}{\bar{V}_i + \delta_1 \bar{V}_1} \tag{30}$$

We can obtain ϕ_i^{coex} rather easily from the tables as it is related to ϕ_{tot}^{coex} by:

$$\phi_i^{coex} = \phi_{tot}^{coex} - \phi_j \quad (i,j = 1,2;\ i \neq j) \tag{31}$$

We have divided our discussion of the effect of variation in protein charge into three separate cases. We first consider the case when the larger protein is charged, while the smaller protein is uncharged. We then discuss the opposite case (charged smaller protein and uncharged larger), and finally we describe the behavior when both proteins are charged.

Table 9. Coexistence Volume Fractions of Total Protein for Precipitation of Protein 1 and 2 as a Function of Protein Mole Fraction and Polymer Volume Fraction for $z_1 = 0$ and $z_2 = 10$

	$\phi_3 = 0.0$				$\phi_3 = 0.10$				$\phi_3 = 0.20$			
	$C_{salt} = 0$		$C_{salt} = 0.3$ M		$C_{salt} = 0$		$C_{salt} = 0.3$ M		$C_{salt} = 0$		$C_{salt} = 0.3$ M	
x_1	pr1	pr2	pr1	pr2	pr1	pr2	pr1	pr2	pr1	pr2	pr1	pr2
0.10	**0.56**	—	**0.56**	—	**0.47**	—	**0.471**	—	**0.309**	—	**0.31**	—
0.30	**0.53**	—	**0.534**	—	**0.442**	—	**0.445**	—	**0.262**	—	**0.265**	—
0.50	**0.52**	—	**0.52**	—	**0.436**	—	**0.439**	—	**0.245**	—	**0.248**	—
0.70	**0.51**	—	**0.515**	—	**0.435**	—	**0.438**	—	**0.236**	—	**0.239**	—
0.90	**0.50**	—	**0.508**	—	**0.436**	—	**0.439**	—	**0.231**	—	**0.234**	—

Boldfaced numbers = protein precipitating at the given protein charges, protein mole fraction and polymer volume fraction
— = no interaction of μ_i/kT vs. p/kT curves

Table 10. Coexistence Volume Fractions of Total Protein for Precipitation of Protein 1 and 2 as a Function of Protein Mole Fraction and Polymer Volume Fraction for $z_1 = 5$ and $z_2 = 5$

	$\phi_3 = 0.0$				$\phi_3 = 0.10$				$\phi_3 = 0.20$				$\phi_3 = 0.30$			
	$C_{salt} = 0$		$C_{salt} = 0.3$ M		$C_{salt} = 0$		$C_{salt} = 0.3$ M		$C_{salt} = 0$		$C_{salt} = 0.3$ M		$C_{salt} = 0$		$C_{salt} = 0.3$ M	
x_1	prl	pr2	prl	pr2	prl	pr2	prl	pr2	prl	pr2	prl	pr2	prl	pr2	prl	pr2
0.10	0.643	**0.625**	0.617	**0.609**	**0.544**	0.562	**0.524**	0.546	**0.398**	0.429	**0.381**	0.418	**0.124**	0.149	**0.089**	0.105
0.30	**0.615**	0.652	**0.593**	0.637	**0.521**	0.595	**0.503**	0.581	**0.35**	0.47	**0.344**	0.462	**0.046**	0.153	**0.037**	0.14
0.50	**0.607**	0.676	**0.588**	0.663	**0.516**	0.629	**0.502**	0.61	**0.34**	0.523	**0.332**	0.511	**0.038**	0.204	**0.024**	0.196
0.70	**0.603**	0.706	**0.585**	0.694	**0.517**	0.676	**0.502**	0.66	**0.334**	0.589	**0.327**	0.576	**0.025**	0.311	**0.018**	0.28
0.90	**0.599**	—	**0.582**	—	**0.519**	—	**0.505**	—	**0.330**	—	**0.330**	—	**0.016**	—	**0.015**	0.48

Boldfaced numbers = protein precipitating at the given protein charges, protein mole fraction and polymer volume fraction
— = no intersection of the μ_i/kT vs. p/kT curves

Tables 6, 7 and 8 show cases of a charged larger protein paired with an uncharged smaller one. We know *a priori* that the size effect will enhance the precipitation of protein 1, and we expect the charge to decrease it. We also know that the relative amounts of each protein in the fluid mixture (mole fractions) affect the solubility characteristics, with the more concentrated protein being more likely to precipitate. Hence, depending on the magnitude of the charge on the protein, the relative amounts of protein 1 and 2 and the concentration of the polymer, we may expect to see a shift in the precipitation behavior. Indeed, this is exactly what is observed. For instance, in Figure 8 we plot the coexistence volume fraction of total protein (total volume fraction of protein at precipitation) vs. the concentration of polymer added. In Figure 8, protein-1 has a charge of 10, while protein-2 is uncharged. We can compare this result with Figure 4a (same diameter ratio) where both proteins are uncharged. In Figures 4a and 8, the protein mole fraction is 0.5 and no salt is added. We see that in Figure 4a, protein 1 precipitates at all polymer concentrations, whereas in Figure 8 (where $z_1 = 10$) it is protein 2 that precipitates. In fact, we see from Table 7 that when $z_1 = 10$ and $z_2 = 0$, protein 2 is predicted to precipitate in preference to protein 1 except at the highest polymer volume fraction ($\phi_3 = 0.30$) and the highest mole fraction of protein 1 ($x_1 = 0.90$). This implies that for this particular set of parameters, the electrostatic effect overrides the size advantage of protein 1.

To check the relative importance of the two effects, we consider systems with less charge on protein 1. The coexistence volume fractions for the case in which $z_1 = 5$ and $z_2 = 0$ are listed in Table 7. In this case, we see more clearly the interplay between the charge, size and concentration effects. In Figure 9a, we plot the coexistence volume fraction vs. the polymer concentration for $z_1 = 5$, $z_2 = 0$ for a mole fraction of protein of 0.3 with added salt concentration of 0.30 M. Figure 9b shows a similar plot for a mole fraction of 0.7. When protein 2 is present in higher amounts than protein 1 (Figure 9a), the theory predicts precipitation of protein 2 at the lower polymer

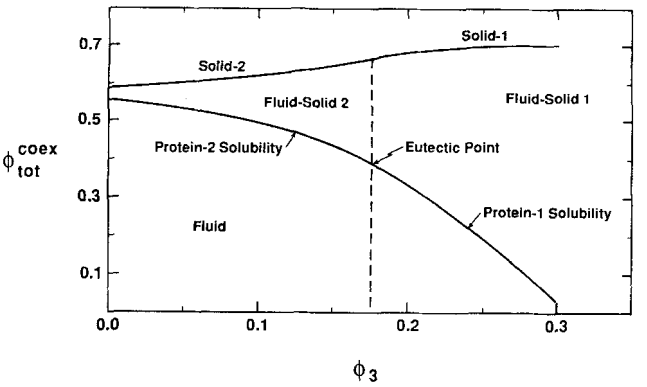

Figure 9a. Total coexistence volume fraction of protein vs. polymer volume fraction added for $z_1 = 5$, $z_2 = 0$, and $x_1 = 0.30$.

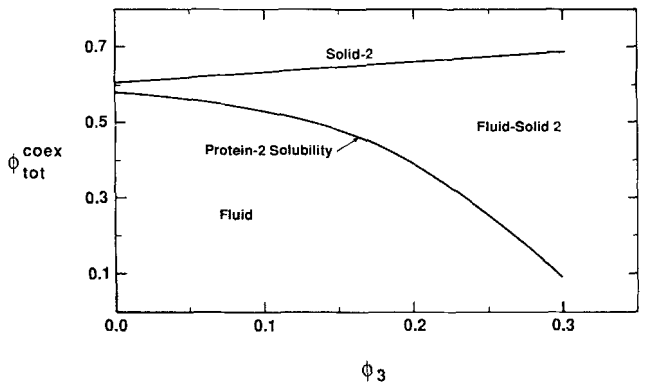

Figure 8. Total coexistence volume fraction of protein vs. polymer volume fraction added for $z_1 = 10$, $z_2 = 0$, and $x_1 = 0.50$.

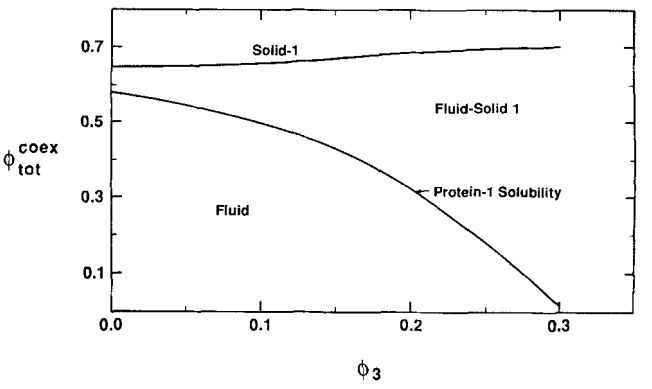

Figure 9b. Total coexistence volume fraction of protein vs. polymer volume fraction added for $z_1 = 5$, $z_2 = 0$, and $x_1 = 0.70$.

concentrations and precipitation of protein 1 at high polymer concentrations. However, for mixtures richer in the larger protein (Figure 9b), the theory predicts precipitation of protein 1, even at the lowest polymer concentrations. Hence, for this set of parameters the system exhibits a rich variety of changes in response to variation in the concentrations of the proteins and polymer. We can unambiguously conclude that a reduction in the protein charge does in fact lead to an increase in its tendency to precipitate as does an increase in protein size and relative concentration. The coexistence values for a case when $z_1 = -5$ and $z_2 = 0$, Table 8, are not much different from the case of $z_1 = 5$ and $z_2 = 0$. This is not unexpected because the only difference in the two cases is the presence of oppositely charged counterions of (slightly) different sizes.

Table 9 shows the results for the case when the charge on the smaller protein is set to 10 and the charge on the larger protein is set to 0. In this case, both the size effect and the charge effect favor the precipitation of the larger (and uncharged) protein. These effects dominate the effect of relative protein concentration, and consequently even when the smaller protein is in excess we predict that the size and charge effects "win out" over the concentration effect and the larger protein precipitates.

Table 10 shows the results for the case of both proteins charged: both proteins bear a charge of 5. Results for this case are qualitatively identical to that of both proteins being uncharged, as discussed earlier. For instance, when both proteins are equally charged as in this case, we find that the larger protein is preferentially precipitated over the smaller one for most of the cases studied (we termed this as a size effect). The exceptions to this rule occur when the smaller protein is in large excess (the concentration effect). We also see that upon addition of polymer, not only is the solubility reduced but also the precipitation of the larger protein become more likely. For example, in Table 10, at the lowest mole fraction of protein 1 studied ($x_1 = 0.10$), protein 2 precipitates at the lowest polymer volume fraction, but any further addition of polymer leads to precipitation of protein 1. All these trends are similar to those for precipitation at the isoelectric point, and we can therefore identify the size, concentration and polymer effects as before.

Finally, we consider the effect of added salt on the solubility behavior, which depends on whether the *precipitating* protein is charged or not. When the precipitating protein is uncharged (for instance, $z_1 = 0.0$ and $z_2 = 10$ in Table 9), we see no perceptible effect of the addition of salt. This agrees with our experimental findings for single-protein precipitation that at the isoelectric point, changing the ionic strength has almost no effect on its solubility (Mahadevan and Hall, 1991). The same behavior is observed for protein 2, when it precipitates and is uncharged (see, for example, the case in which $z_1 = 10$ and $z_2 = 0$ in Table 6). However, for a case when the precipitating protein is charged, ($z_1 = 5$ and $z_2 = 5$ in Table 10), for every mole fraction and polymer volume fraction, addition of salt leads to a reduction in the solubility of both proteins. Figure 10 shows the total coexistence volume fraction of protein vs. the volume fraction of polymer added for a protein mole fraction of 0.5. The addition of salt to 0.3 M (increase in ionic strength) slightly reduces the coexistence protein concentration for every polymer concentration. Equivalently, we can say that the amount of polymer that needs to be added to

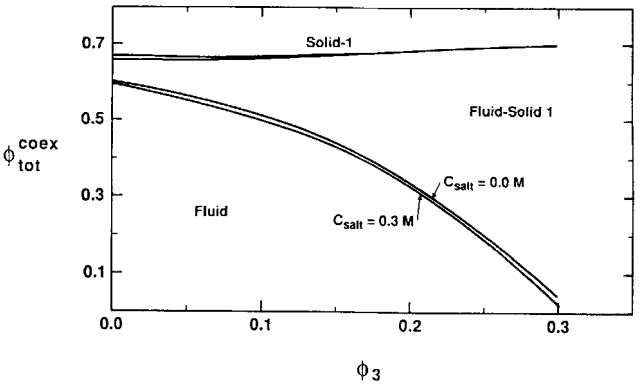

Figure 10. Effect of added salt on the total coexistence volume fraction of protein for $z_1 = 5$, $z_2 = 5$, and $x_1 = 0.50$.

precipitate a protein out of a mixture decreases with increase in ionic strength. Even though the magnitude of this decrease appears to be quite small, the effect on the solubility is magnified, because as in Eq. 30 the small difference in the coexistence volume fraction is magnified by three orders of magnitude in the solubility difference. The reduction in the solubility with increasing salt concentration is seen for all protein mole fractions (see Table 10).

Conclusion

We have examined the relative importance of protein and polymer size and concentrations and protein charge on the precipitation of proteins by nonionic polymer. Size is the most important criterion in determining which protein will precipitate under a given set of conditions. We find that the charge on the protein can also play a significant role in determining the solubility behavior of proteins in a mixture. We also have studied the case of two similar-sized (not same) proteins to reduce the important role played by size in determining which protein precipitates. For the diameter ratio of 6:5:1 (protein 1:protein 2:polymer), which we have examined earlier under no-charge conditions, significantly different phase behavior can be obtained depending on the charge of both proteins. An increase in protein charge reduces its ability to precipitate, while all other parameters such as protein size, mole fraction, and polymer concentration are kept constant.

Acknowledgment

The authors gratefully acknowledge the support of the National Institutes of Health (Grant #1 RO 1-GM40023-03), the National Science Foundation (Grant #CBT-8720284), and the North Carolina Biotechnology Center. We also acknowledge Dr. Ronald Dickman for permission to reproduce the derivation of the intermolecular potential. One of the authors (HM) acknowledges Dr. Al Post for helpful discussions relating to the evaluation of the radial distribution function of hard-sphere mixtures. Finally, we would like to thank Dr. Daniel Forciniti, Dr. Rainer Czech, and Dr. Arun Yethiraj for their helpful discussions during the preparation of this work.

Notation

A = Helmholtz free energy
$c_{ij}(r)$ = direct correlation function between species i and j
d = diameter of a molecule

e = electronic charge
$g_0^{ij}(r)$ = radial distribution function between species i and j
$h_{ij}(r)$ = total correlation function between species i and j
k = Boltzmann's constant
M_i = molecular weight of protein i
n_3 = number density of polymer molecules based on available volume
N = number of molecules in system
N_{Av} = Avogadro's number of molecules
p = pressure
r = intermolecular distance
S_i = solubility of protein i
T = absolute temperature
$u_{ii}(r)$ = intermolecular pair potential between like species
$u_{ij}(r)$ = intermolecular pair potential between unlike species
V = volume of system
$\overline{V}_1$ = inverse specific density of solvent
$\overline{V}_i$ = partial specific volume of protein i
x_i = mole fraction of species i
z_i = charge on species i

Greek letters

β = dimensionless temperature $(1/kT)$
γ_i = activity coefficient of species i
Γ = universal scaling parameter
δ_1 = hydration of protein
ϵ_0 = dielectric constant of continuum
κ = Debye length
μ_i = chemical potential of species i
Π = osmotic pressure
ϕ_0 = close-packed volume fraction, $(\pi/6)\sqrt{2} = 0.74$
ϕ_i = volume fraction of species i
ρ_i = number density of species i

Subscripts

1 = protein 1
2 = protein 2
3 = polymer
4,5 = counterions
6,7 = added salt
hs = hard sphere
tot = total

Superscripts

coex = coexistence
elec = electrostatic
vex = volume exclusion

Literature Cited

Asakura, S., and F. Oosawa, "Interaction between Particles Suspended in Solutions of Macromolecules," *J. Poly. Sci.*, **33**, 183 (1958).

Atha, D. H., and K. C. Ingham, "Mechanism of Precipitation of Proteins by Polyethylene Glycols," *J. Biol. Chem.*, **256**, 12108 (1981).

Ballone, P., G. Pastore, and G. Galli, "Additive and Nonadditive Hard-Sphere Mixtures," *Molec. Phys.*, **59**(2), 275 (1975).

Bjurstrom, E., "Biotechnology: Fermentation and Downstream Processing," *Chem. Eng.*, **92**(4), 151 (1985).

Blum, L., "Mean Spherical Model for Asymmetric Electrolytes: 1. Method of Solution," *Molec. Phys.*, **30**, 1529 (1975).

Blum, L., and J. S. Hoye, "Mean Spherical Model for Asymmetric Electrolytes: 2. Thermodynamic Properties and the Pair Correlation Function," *Molec. Phys.*, **35**, 299 (1978).

Burden, R. L., J. D. Faires, and A. C. Reynolds, *Numerical Analysis*, PWS Publishers, Boston, MA (1981).

Cantor, C. R., and P. R. Schimmel, *Biophysical Chemistry: 2*, W. H. Freeman and Co. (1980).

Carnahan, N., and K. Starling, "Thermodynamic Properties of a Rigid-Sphere Fluid," *J. Chem. Phys.*, **53**, 600 (1970).

de Hek, H., and A. Vrij, "Interactions in Mixtures of Colloidal Silica Spheres and Polystyrene Molecules in Cyclohexane," *J. Coll. Interf. Sci.*, **84**, 409 (1981).

Dickman, R., personal communication (1988).

Edmond, E., and A. G. Ogston, "An Approach to the Study of Phase Separation in Ternary Aqueous Systems," *Biochem. J.*, **109**, 569 (1968).

Findlay, A., A. N. Campbell, and N. O. Smith, *The Phase Rule and Its Applications*, 9th ed., Dover Publications, New York (1951).

Foster, P. R., P. Dunnill, and M. D. Lilly, "The Precipitation of Enzymes from Cell Extracts of *Saccharomyces Cerevisiae* by Polyethylene Glycol," *Biochim. Biophys. Acta*, **317**, 505 (1973).

Fries, P. H., and J. P. Hansen, *Molec. Phys.*, **48**, 8891 (1983).

Gast, A. P., C. K. Hall, and W. G. Russell, "Polymer-Induced Phase Separations in Nonaqueous Colloidal Suspensions," *J. Coll. Interf. Sci.*, **96**, 251 (1983).

Hall, K. R., "Another Hard-Sphere Equation of State," *J. Chem. Phys.*, **57**, 2252 (1971).

Haire, R. N., W. A. Tisel, J. G. White, and A. Rosenberg, "On the Precipitation of Proteins by Polymers: The Hemoglobin-Polyethylene Glycol System," *Biopoly.*, **23**, 2761 (1984).

Hiroike, K., "Supplement to Blum's Theory for Asymmetric Electrolytes," *Molec. Phys.*, **33**, 1195 (1977).

Hönig, W., and M. R., Kula, "Selectivity of Protein Precipitation with PEG Fractions of Various Molecular Weights," *Anal. Biochem.*, **72**, 502 (1976).

Ingham, K. C., "Polyethylene Glycol in Aqueous Solution: Solvent Perturbation and Gel Filtration Studies," *Arch. Biochem. Biophys.*, **184**; "Precipitation of Protein with PEG: Characterization of Albumin," **59** (1977), *ibid.*, **186**, 106 (1978).

Ingham, K. C., Personal communication (1990).

Knoll, D., and J. Hermans, "Polymer-Protein Interactions," *J. Biol. Chem.*, **258**, 5710 (1983).

Kula, M. R., W. Hönig, and H. Foellmer, *Proc. Int. Workshop on Technol. for Protein Separation and Improvement of Blood Plasma Fractionation*, H. E. Sandberg, ed., National Institutes of Health, Bethesda, MD, DHEW Publication, No. NIH78-1422 (1977).

Kula, M. R., personal communication (1991).

Leonard, P. J., D. Henderson, and J. Barker, "Calculation of the Radial Distribution Function of Hard-Sphere Mixtures in the Percus-Yevick Approximation," *Trans. Farad. Soc.*, **66**, 2439 (1970).

Mahadevan, H., and C. K. Hall, "A Statistical-Mechanical Model of Protein Precipitation by Nonionic Polymer," *AIChE J.*, **36**(10), 1517 (1990).

Mahadevan, H., and C. K. Hall, "A Systematic Experimental Study of Protein Precipitation by Nonionic Polymer," *Fluid Phase Equil.*, in press (1992).

Mansoori, G. A., N. F. Carnahan, K. E. Starling, and T. W. Leland, Jr., "Equilibrium Thermodynamic Properties of the Mixture of Hard Spheres," *J. Chem. Phys.*, **54**(4), 1523 (1971).

McMillan, W. G., and J. E. Mayer, "The Statistical Thermodynamics of Multicomponent Systems," *J. Chem. Phys.*, **13**, 276 (1945).

McQuarrie, D. L., *Statistical Mechanics*, Harper and Row, New York (1976).

Middaugh, C. R., W. A. Tisel, R. N. Haire, and A. Rosenberg, "Determination of the Apparent Thermodynamic Activities of Saturated Protein Solutions," *J. Biol. Chem.*, **254**(2), 367 (1979).

Ogston, A. G., and C. F. Phelps, "The Partition of Solutes Between Buffer Solutions and Solutions Containing Hyaluronic Acid," *Biochem. J.*, **78**, 827 (1961).

Ogston, A. G., "Some Thermodynamic Relationships in Ternary Systems, with Special Reference to the Properties of Systems Containing Hyaluronic Acid," *Arch. Biochem. Biophys. Suppl.*, **1**, 39 (1962).

Perram, J. W., "Hard Sphere Correlation Functions in the Percus-Yevick Approximation," *Molec. Phys.*, **30**(5), 1505 (1975).

Polson, A., G. M. Potgeiter, J. F. Largier, G. E. F. Mears, and F. H. J. Joubert, "The Fractionation of Protein Mixtures by Linear Polymers of High Molecular Weight," *Biochim. Biophys. Acta*, **82**, 463 (1964).

Sandler, S., *Chemical and Engineering Thermodynamics*, 2nd ed., Wiley, p. 480 (1988).

Scopes, R., *Protein Purification*, Springer Verlag, New York (1982).

Triolo, R., J. R. Grigera, and L. Blum, "Simple Electrolytes in the

Mean Spherical Approximation," *J. Phys. Chem.*, **17**, 1858 (1976).
Vericat, F., and J. R. Grigera, "Theoretical Single-Ion Activity of Calcium and Magnesium Ions in Aqueous Electrolyte Mixtures," *J. Phys. Chem.*, **86**, 1030 (1982).
Weis, J. J., and J. M. Kincaid, "Radial Distribution Function of a Hard-Sphere Solid," *Molec. Phys.*, **34**, 931 (1977).

Appendix: Effective Interaction between Particles in a Background Fluid

We reproduce the derivation for the volume-exclusion potential, which was originally done by Dickman (1988), for a binary mixture of proteins in a background fluid.

Consider a pair of particles (1,2) at r_1 and r_2 with a pair potential $u_0(r)$, immersed in a "background fluid." This fluid is assumed to consist of a large number N, of identical "b-particles." The partition function of the $2+N$ body system is:

$$\mathcal{Z}(2,N,\nu,\beta)=\int_{r_i,x_i\in\nu} dr_1 dr_2 \int dx_1 \ldots dx_N$$

$$\exp\left\{-\beta\left[u_0(r)+\sum_j\left(u_b^{(1)}(|r_1-x_j|)\right.\right.\right.$$

$$\left.\left.\left.+u_b^{(2)}(|r_2-x_j|+\sum_{i<j}u_{bb}(x_{ij}))\right)\right]\right\} \tag{A1}$$

where β is $1/kT$, ν is the region occupied by the particles, x_i are the b-particle coordinates, u_b^i is the interaction between particle i and a b-particle and u_{bb} is the interaction between b-particles.

If we define, for the purposes of computing thermodynamic properties, an effective potential:

$$u_e(r)=$$

$$-\frac{1}{\beta}\log\left\{\int dx_1\ldots dx_N \exp\left(-\beta\left[\sum_j\{u_b^{(1)}(|r_1-x_j|)\right.\right.\right.$$

$$\left.\left.\left.+u_b^{(2)}(|r_2-x_j|)\}+\sum_{i<j}u_{bb}(x_{ij})\right]\right)\right\} \tag{A1}$$

then Eq. A2 can be rewritten as

$$\mathcal{Z}(2,N,\nu,\beta)=\int_{r_i\in\nu} dr_1 dr_2 \exp\{-\beta[u_0(r)+u_e(r)]\} \tag{A2}$$

With this definition, the b-particles no long appear explicitly in $\mathcal{Z}$. We can evaluate the effective potential $u_e(r)$ exactly, if we treat the b-particles as mutually noninteracting. Also, if $u_b^{(i)}(r)$ is an excluded-volume interaction:

$$u_b^i(y)=\begin{matrix}+\infty, & y\in\nu_i\\ 0, & y\notin\nu_i\end{matrix}\qquad i=1,2 \tag{A3}$$

where ν_i is a region excluded by particle i from occupation by a b-particle. In this case we have:

$$u_e(r)=-\frac{1}{\beta}\log\left[\int_{x_i\in\nu;x_i\notin\nu_1\cup\nu_2}\ldots\int dx_1\ldots dx_N\right] \tag{A4}$$

The b-particles are excluded from the union of the exclusion volumes of particles 1 and 2. The total volume accessible to a b-particle is $V+V_{\text{int}}(r)$, where V is the volume of ν less v_1+v_2 (the exclusion volumes of 1 and 2), and $V_{\text{int}}(r)$ is the volume of region of overlap between the exclusion volumes when the particles are separated by a distance r. Hence,

$$\int_{x_i\in\nu;x_i\notin\nu_1\cup\nu_2}\ldots\int dx_1\ldots dx_N=[V+V_{\text{int}(r)}]^N \tag{A5}$$

Setting $u_e=0$ for large $r(V_{\text{int}}(r)=0)$, we have:

$$u_e(r)=-\frac{1}{\beta}\log\left[1+\frac{V_{\text{int}}(r)}{V}\right]^N$$

$$=kTn_3V_{\text{int}}(r) \tag{A6}$$

where $n_3=N/V$ is the density of b-particles. It remains only to compute $V_{\text{int}}(r)$ for specific geometries.

Consider two particles that exclude b-particles from spheres of radii ζ_1 and ζ_2, respectively. The particles are hard spheres of radius a_i and $\zeta_1=a_i+r_g$, where r_g is the radius of a b-particle. We require $V_{ij}(r)$, the volume of overlap of spheres ζ_1 and ζ_2, whose centers are separated by a distance r.

From Figure A1,

$$V_{\text{int}}=\pi\zeta_1^3\int_0^{\theta_1}\sin^3\theta d\theta+\pi\zeta_2^3\int_0^{\theta_2}\sin^3\theta d\theta \tag{A7}$$

This can be written as:

$$V_{\text{int}}=\pi\zeta_1^3\int_{\cos\theta_1}^1(1-u^2)du+\pi\zeta_2^3\int_{\cos\theta_2}^1(1-u^2)du \tag{A8}$$

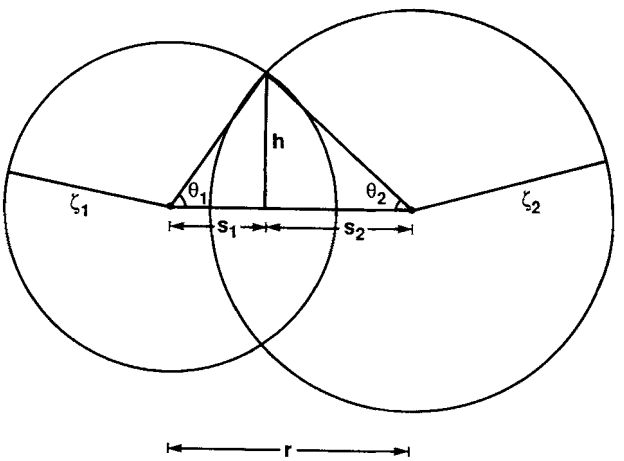

Figure A1. Model for the interaction between two particles in a background fluid.

We know that $S_2^2 - S_1^2 = \zeta_2^2 - \zeta_1^2$ (since $h^2 = \zeta_1^2 - S_1^2 = \zeta_2^2 - S_2^2$). Also, $S_1 + S_2 = r$. Solving these two equations for S_1 and S_2 leads to:

$$S_1 = \frac{r}{2} - \frac{\zeta_2^2 - \zeta_2^2}{2r} \qquad S_2 = \frac{r}{2} + \frac{\zeta_2^2 - \zeta_2^2}{2r} \tag{A9}$$

Noting that $\cos\theta_1 = (S_1/\zeta_1)$ and $\cos\theta_2 = (S_2/\zeta_2)$ leads to the following expression for V_{int}:

$$V_{\text{int}} = \pi\left\{\zeta_1^3\left[1 - \frac{S_1}{\zeta_1} - \frac{1}{3}\left(1 - \frac{S_1^3}{\zeta_1^3}\right)\right] + \zeta_2^3\left[1 - \frac{S_2}{\zeta_2} - \frac{1}{3}\left(1 - \frac{S_2^3}{\zeta_2^3}\right)\right]\right\} \tag{A10}$$

This can be rearranged to give the final expression for V_{int}

$$V_{\text{int}} = \pi\left\{\frac{2}{3}(\zeta_1^3 + \zeta_2^3) + \frac{r^3}{12} - \frac{(\zeta_1^2 + \zeta_2^2)}{2}r - \frac{(\zeta_1^2 - \zeta_2^2)^2}{4r}\right\} \tag{A11}$$

Insertion of Eq. A11 into Eq. A6 then gives us an expression for the volume exclusion potential (see also Eq. 2):

$$\frac{u_e(r)}{kT} = -\frac{2\pi(\zeta_1^3 + \zeta_2^3)n_3}{3}\left\{1 + \frac{r^3}{8(\zeta_1^3 + \zeta_2^3)} - \frac{3}{4}\left(\frac{\zeta_1^2 + \zeta_2^2}{\zeta_1^3 + \zeta_2^3}\right)r - \frac{3}{8r}\left[\frac{(\zeta_1^2 + \zeta_2^2)^2}{\zeta_1^3 + \zeta_2^3}\right]\right\} \tag{A12}$$

As a check of this derivation if we let $\zeta_1 = \zeta_2$ we recapture the Asakura-Oosawa volume-exclusion potential for $u_e(r)$. A further check on Eq. A12 is if we let $r = \zeta_2 - \zeta_1$, $V_{\text{int}} = (4/3)\pi r^3$ as expected. Also, for $r = \zeta_1 + \zeta_2$, we get the correct result, $V_{\text{int}} = 0$.

Manuscript received Oct. 4, 1992.